CONSOLIDATION AND WAVE PROPAGATION IN A POROUS MEDIUM

by

Vladimir Gerasik

A thesis
presented to the University of Waterloo
in fulfillment of the
thesis requirement for the degree of
Master of Mathematics
in
Applied Mathematics

Waterloo, Ontario, Canada, 2006

I hereby declare that I am the sole author of this thesis. This is a true copy of the thesis, including any required final revisions, as accepted by my examiners.

I understand that my thesis may be made electronically available to the public.

Abstract

Basic diffusion analytical solutions of one-dimensional consolidation are presented for the case of a semi-infinite domain. Typical tractions considered include instantaneous loads of the medium with a free boundary pressure, as well as the case of a permeable membrane located at the forced boundary.

Two-dimensional boundary value problems for a porous half-space, described by the widely recognized Biot's equations of poroelasticity, including inertia effects is discussed. In this poroelastic version of Lamb's problem in the classical theory of linear elastic waves, the surface of a porous half-space is subjected to a prescribed line traction. The following two broadly applicable cases are considered: 1) A steady state harmonic load, 2) An impulsive load (Dirac delta function time dependence). A general analytical solution of the problem in the Fourier – Laplace space was obtained by the application of the standard Helmholtz potential decomposition, which reduces the problem to a system of wave equations for three unknown potentials, which correspond to three types of motion: P1, slow P2 wave, and the shear wave S. The possibilities of, and procedure for, obtaining analytic solutions in the physical space subsequently are discussed in detail. When viscous dissipation effects are taken into account, a steady-state harmonic line traction solution can be represented in the form of well convergent integrals, while for the case when viscous dissipation is ignored, closed form analytic solutions can be obtained for impulsive forcing with the application of the Cagniard – de Hoop inversion technique. Numerical studies of the dispersion relation of the Rayleigh, or surface, wave for cases in which the dissipation is not negligible are presented.

Acknowledgments

I would like to thank my supervisor Marek Stastna for numerous discussions and encouragement during preparation and writing of this thesis. Thanks to Arnold Verruijt for his comments on the effective stress concept.

Contents

List of Figures

Chapter 1

Introduction

Poroelasticity is a continuum theory for the analysis of a porous medium consisting of an elastic matrix containing interconnected fluid-saturated pores. Porous media are, by their essence, composite and multiphase. Composite because the solid fraction - the skeleton - is formed of grains whose chemical or crystalline features are often different and multiphase because this solid fraction is always associated with a gas or liquid phase that occupies the voids between the grains. This microscopic heterogeneity of the porous medium induces a complex macroscopic physical behavior sensitive to slight variations in fluid content or of the solid structure. Mathematical models of the porous medium are intended to characterize the material behavior, balancing between the rigor of the laws of mathematical mechanics and the natural disorder of the porous medium. The task is difficult, but the study is motivated by the importance of the applications for which even partial result can lead.

Porous media theory is currently applied in a surprisingly large number of applications. First of all, the ideal area of application is geophysics. While petroleum geophysics or petrophysics, due to its economic importance, appears to monopolize the field of potential applications, one should not minimize the importance of other applications such as rock mechanics, soil mechanics and hydrogeology.

Soil mechanics is an important discipline for many branches of engineering, such as Civil engineering, Geotechnical engineering and Engineering geology. It is used in the design of foundations to support structures, embankments, retaining walls, earthworks and underground openings. The percolation of water through soils is of importance in the construction of tunnels and deep foundations, and obviously water-related structures such as bridge pilings and dams.

Hydrogeology or geohydrology is the part of hydrology that studies the occurrence and movement of water beneath the earth's surface (groundwater) and deals with chemical and physical interactions between soil and water. Groundwater is any water found below the land surface. It is found in aquifers, in the pore spaces of rocks, in unconsolidated sediments, such as permafrost, and as soil moisture.

For the area of biomechanics, which studies the mechanical properties of human tissues, the theory of porous media plays a significant role as a mathematical foundation. For example, brain or bone tissue can be represented as a porous material infiltrated by cerebrospinal fluid or blood, respectively.

The presence of the freely moving fluid in a porous structure modifies its mechanical response. Two mechanisms play a key role in this interaction between the interstitial fluid and porous rock: (i) an increase of pore pressure induces a dilatation of the skeleton (or solid matrix), and (ii) compression of the skeleton causes a rise of pore pressure, if the fluid is prevented from escaping the pore network. These coupled mechanisms reveal the time-dependent character of the mechanical properties of the material. Generally speaking, all possible areas of application demonstrate two basic phenomena of poroelastic behavior: solid-to-fluid coupling and fluid-to-solid coupling. *Solid-to-fluid* coupling occurs when a change in applied stress produces a change in fluid pressure or fluid mass contained in the porous matrix, while *fluid-to-solid* coupling occurs when a change in fluid pressure or fluid mass is responsible for a change in the volume of the porous material.

The application of the theory has generally concerned quasi-static (or consolidation) problems and wave propagation (or dynamic problems). The earliest theory to account for the influence of pore fluid on the quasi-static deformation of soils was developed in 1923 by Terzaghi [44] who proposed a model of one-dimensional consolidation. In 1941 it was generalized for three dimensional problems by Biot [4] and was intensively adopted for the solution of the various geotechnical problems and soil mechanics [46]. Later, quasi-static linear theory of poroelasticity was modified by Biot himself in his fundamental work [6] to include both basic interaction mechanisms: inertia and viscous dissipation. Biot's equations, [6], [7], [9] give the most general mathematical description of the porous medium adopted today for analysis of wave propagation in porous media.

One of the most interesting features of Biot's theory is the propagation of a second compressional wave. In 1956 Biot, following Frenkel, noted the existence and studied the properties of the P2 slow wave in porous media [6], however, due to experimental difficulty, this wave was first observed only in 1980, in studies of water-saturated sintered glass beads at ultrasonic frequencies conducted by Plona [37], [9]. Extensive quantitative experimental research on this kind of porous ma-

terials shows the strong predictive power of Biot's theory and confirms the attenuation mechanism involved. For example, recently, experimental data of slow wave propagation in natural water-saturated sandstone under atmospheric conditions at ultrasonic frequencies was presented in [25]. Certain attempts have been made to use slow compressional waves to determine reservoir permeability for petrophysical purposes [35]. On the other hand, the question of why slow Biot's wave can not be experimentally detected in low-permeability materials such as natural rocks is one of the major issues in the acoustics of fluid-saturated porous media [30]. Indeed, detailed studies of three wave types (dilatational P1, P2 and shear S) conducted by Biot [6] show that the velocity is observed to rise with increasing frequency, however, the more highly attenuated character of the slow wave, in comparison with the other two, leads to the paradoxical situation: the more likely the phenomenon is to occur, due to the velocity increasing as the frequency increases, the more the wave in question will be attenuated.

Wave propagation and, in particular, surface, or Rayleigh, waves were studied extensively since Deresiewicz [13] first described surface waves for the open pore case. It was shown that the surface wave has components of all three bulk waves. Based on the dynamical Biot's theory, problems of estimation of wave propagation are mainly studied analytically, for instance, [11], [15], [20], [22], [43], [27], numerically [40], [28], and experimentally [25], [30]. Less attention has been paid to the solution of boundary value problems [41], [14], [33], [19], [23], [29], due to their complexity. Mostly, steady-state (with oscillatory sources) boundary value problems were considered for the cases when dissipation is neglected [14], [33], [43]. In [23], [45], [36] the steady-state poroelastic version of the axisymmetric Lamb's problem [26] was considered for a dissipative medium. Transient wave propagation studies, whose results can hardly be overestimated, were covered in comparatively fewer works [41], [33], [19], [29], recent numerical results can be found in [40], [28].

It is important to stress that Biot's theory is not the only existing mathematical description of porous continua. Among other theories, two theories are rapidly developing: Wilmanski's theory (see [48], [15], [2]) and the so-called, "theory of porous media" (or TPM) (see [12], [39] for references). While Biot's theory is based on the works of von Terzaghi [44], TPM was developed following the ideas of Fillunger. Recently, Shantz [39] analyzed, numerically, the one dimensional problem of a poroelastic column to demonstrate inconsistencies between the two theories. It was shown, that results agree perfectly for the case of incompressible constituents, but that a great discrepancy can be observed for the case of compressible constituents. This is caused by the different assumptions for the fluid motion in both theories.

3

Wilmanski's theory is similar to Biot's theory and can be considered as a simplified Biot's theory (less pronounced coupling) with the additional equation of porosity balance. Thus, this theory inherits the main features of Biot's theory, namely the P2 slow wave (Biot's effect) [48], [15], [2]. Interestingly, Nagy [30] pointed out that experimentally, the slow P2 wave can not be observed in rock structures at low frequencies, while recent studies Edelman [15] show that for Wilmanski's theory, P2 wave is not propagating below a certain wave number. On the other hand, analysis of the wave propagation based on TPM theory [12] reveals only one dilatational wave.

Summarizing, it can be noted that boundary value problems are more extensively studied for the Biot's theory (as it appeared exactly fifty years ago) including extensive recent studies of the surface Stoneley wave on the interface between porous medium and fluid [19], [22]. For the more recent Wilmanski theory not a single boundary problem yet been solved, however, recently, the secular equation for the surface wave was presented and analyzed by Albers and Wilmanski [2]. For TPM, boundary value problems are also yet very much *terra incognita*. Regarding surface waves, recent work of Liu and de Boer [27] (see also [12]) should be mentioned. In this work dispersion relation for Rayleigh waves was obtained and phase velocities as well as attenuations were analyzed.

The present work is organized in the following way: Chapter 2 provides the description of the mathematical models (Biot's theory and consolidation theory), Chapter 3 contains the simple 1D consolidation solutions to illustrate the main concepts of consolidation theory, Chapter 4 is dedicated to the wave propagation problems in porous medium.

Chapter 2

Model Description

2.1 Preliminaries

As a necessary preliminary to a presentation of the constitutive equations, mass and momentum conservation laws, basic kinematic and dynamic quantities that are used in the mechanical description of a saturated porous material will be introduced.

Porosity, by definition, is the ratio of the pore volume V_P to the total volume V_T of the considered body:

$$\phi = \frac{V_P}{V_T}.$$
(2.1)

There is a variety of methods for measuring porosity [9]. If the solid volume is given by $V_S = V_T - V_P$ it is sufficient to obtain two of these three parameters to calculate porosity. For example, for sedimentary rocks typical porosities may vary from 20% (kaolinitic sandstone) to 44% (bioclastic limestone).

The filtration velocity vector $\dot{\mathbf{w}}$, by definition, is given by

$$\dot{\mathbf{w}} = \phi \left(\dot{\mathbf{U}} - \dot{\mathbf{u}} \right),$$
(2.2)

where $\mathbf{u}$ and $\mathbf{U}$ are the mean displacements of the continuous solid and fluid phase, respectively, and a superimposed dot denotes time derivative. In this case, the local increase in fluid content ξ is given by

$$\xi = - \operatorname{div} \mathbf{w}.$$
(2.3)

Permeability of the porous medium k, first defined by Darcy, quantifies the proportion of the flow rate per unit area to the pressure drop in the porous body. Darcy's law (1856) [9], [46] in its simplest steady-state form for the isotropic case can be written in the following form:

$$\dot{\mathbf{w}} = -\frac{k}{\eta} \operatorname{grad} p, \tag{2.4}$$

where η is the kinematic viscosity of the fluid and p is the pore pressure. Permeability is treated as an area, hence its unit in the International System is m². The traditional unit of permeability is the darcy (D), which is equivalent to the square micron (1 darcy is exactly equal to 0.986923 μm²), but the millidarcy (mD) ($\cong 10^{-15}$ m²) is often used, as it is better adapted to the order of magnitude of the permeability scales observed in nature. Sometimes, it is convenient to introduce the hydraulic permeability, or mobility, in the form:

$$K = \frac{k}{\eta}. \tag{2.5}$$

As an example, for sedimentary rocks permeability k takes the range from 6 mD (white chalk) to 7000mD (dedolomitized limestone).

The macroscopic strain tensor, assuming small displacements both for the fluid and solid phase, can be written down to second order:

$$\varepsilon_{ij} = \frac{1}{2} \left(u_{i,j} + u_{j,i} \right), \tag{2.6}$$

where u_i is the ith component of the mean macroscopic displacement. This assumption is fully satisfied, as, for example, the strains in seismic studies (laboratory or field) are less than 10^{-6}.

2.1.1 Darcy's law

Darcy's equation (2.4) is only true for low Reynolds numbers or for the regions where the velocity is not too large. In the range of validity of Darcy's law, i.e., $Re < 1$ (or even <10), the viscous forces that resist the flow are dominant and inertia is ignored. As the flow velocity increases, a gradual transition is observed from inertia-free laminar flow, to flow that is still laminar, but for which inertial forces must be taken into account. Often, the value of $Re = 100$ is mentioned as the upper limit of this transition region in which Darcy's linear law is no longer

valid. For more complicated models and some special cases, Darcy's law has been reformulated several times [6], [10], [34].

For flow in this range, the motion equation, known as *Darcy–Forchheimer's equation*, is used. For a rigid porous medium, neglecting the effects of inertia at the macroscopic level, it takes the form (Forchheimer, 1901) [34]:

$$\frac{\eta}{k}\dot{\mathbf{w}} + a\,|\dot{\mathbf{w}}|\,\dot{\mathbf{w}} + b\,|\dot{\mathbf{w}}|^2\,\dot{\mathbf{w}} = -\operatorname{grad}p, \qquad (2.7)$$

where a and b are the coefficients, related to the configuration of the void space. At low Re, the second and the third terms on the right hand side (2.7), which express the average of the microscopic inertial effects, become negligible, and the equation reduces to the linear Darcy's law. This formulation is very important for petroleum engineering in situations when the fluid discharge is considered in the neighborhood of bore holes. In this situation viscous effects no longer dominate and the description of the flow becomes strongly non-linear.

For example, when all inertial effects are negligible, but we do not neglect the dissipation of energy within the fluid, as fluid layers move at different velocities, the equation of motion takes the form known as *Brinkman's equation* (Brinkman, 1948) [10]:

$$\dot{\mathbf{w}} = -\frac{k}{\eta}\left(\operatorname{grad}p + \lambda\triangle\dot{\mathbf{w}}\right), \qquad (2.8)$$

where λ is an effective viscosity and $\triangle$ is the Laplace operator. The correction term $\lambda\triangle\dot{\mathbf{w}}$ accounts for flow through medium where the grains of the media are porous themselves. This equation is difficult to use, and the correction term is typically neglected.

Very important results, connecting pore pressure and fluid discharge, were obtained by Biot [7], [6]. The generalization of Darcy's law for non-steady flow is known as Biot's equation:

$$-\operatorname{grad}p = \rho_{uw}\ddot{\mathbf{u}} + \rho_w\ddot{\mathbf{w}} + \frac{\eta}{k}\dot{\mathbf{w}}, \qquad (2.9)$$

where ρ_{uw}, ρ_w - are reference phase densities, which will be identified subsequently.

2.2 Model description

Assumptions

1. Porous medium consists of two continuous interacting phases - solid skeleton (or solid matrix) and, possibly gas saturated, pore fluid. The solid skeleton is represented by a matrix of solid grains, which are incompressible themselves, however compression of the solid skeleton is possible and occurs by rearranging the solid particles. Change of pore pressure causes compression or tension in the pore fluid and stimulates fluid flow inside the pores. It should be mentioned, that for Terzaghi theory mechanical properties of the solid skeleton are preserved and do not depend on fluid motion and saturation character. They are totally determined by the stresses arising in the solid matrix. That is why the term "effective stress" is used to describe stresses in the solid skeleton.

2. Size of pores is small, compared to the distance on which kinematic and dynamic characteristics of the motion change. In other words, the wavelength is large in comparison with the dimension of the elementary channels where microscopic flow occurs.

3. There are no phase transitions in the porous medium.

4. Deformations and displacements of both solid and fluid phases are small.

5. The gas constituent is totally dissolved in the pore fluid and influences both the density and bulk modulus of the pore fluid.

6. The solid matrix is assumed to be elastic and isotropic, hence all the mechanisms of viscous origin related to the matrix are neglected.

7. Fluid viscosity is only accounted for in inter-phase interactions.

8. Temperature effects are not considered.

2.2.1 Biot's Model

Constitutive equations of a porous medium can be obtained in several ways: either they can be established from the main principles of continuum mechanics, using energy considerations and introducing a volumetric dissipation function, or using the equations of a multiphase mixture, limiting the number of constituents to two and prescribing characteristics of interphase correlation [41].

However, the classical approach, used by Biot [7], [9] was based on the introduction of an internal volumetric potential $\mathbf{V}$, such that its differential represents the deformation work done for an infinitesimal macroscopic transformation:

$$\mathrm{d}\,\mathbf{V} = \frac{\partial \mathbf{V}}{\partial \varepsilon_{ij}}\,\mathrm{d}\,\varepsilon_{ij} + \frac{\partial \mathbf{V}}{\partial \xi}\,\mathrm{d}\,\xi, \tag{2.10}$$

where the summation applies to the repeated subscripts and ξ is the variation of the fluid content (2.3).

The first term on the right hand side (2.10) corresponds to the elementary deformation work at fixed fluid content, and the second is associated with the increase in fluid content at fixed macroscopic deformation. Hence, it is reasonable to define a macroscopic stress tensor σ_{ij} and a mean pressure in the pore fluid p by

$$\sigma_{ij} = \frac{\partial \mathbf{V}}{\partial \varepsilon_{ij}}, \qquad p = \frac{\partial \mathbf{V}}{\partial \xi}. \tag{2.11}$$

Assuming small disturbances, the expansion of $\mathbf{V}$ can be limited to the quadratic terms. The assumption of isotropy implies that this expansion only involves the first two invariants of the strain tensor, $\mathbf{I}_1 = \mathrm{tr}\,\varepsilon$ and $\mathbf{I}_2 = 2\left(\mathrm{tr}\,(\varepsilon^2) - (\mathrm{tr}\,\varepsilon)^2\right)$ as well as the variation of fluid contents ξ. Therefore

$$2\mathbf{V} = (\lambda_f + 2\mu)\mathbf{I}_1^2 + \mu\mathbf{I}_2 - 2\beta M \mathbf{I}_1 \xi + M\xi^2. \tag{2.12}$$

From (2.11) and (2.12) it can be inferred that

$$\begin{aligned} \sigma_{ij} &= \lambda_f \,\mathrm{tr}\,\varepsilon\delta_{ij} + 2\mu\varepsilon_{ij} - \beta M \xi \delta_{ij}, \\ p &= M(-\beta\,\mathrm{tr}\,\varepsilon + \xi), \end{aligned} \tag{2.13}$$

or alternatively,

$$\begin{aligned} \sigma_{ij} &= \lambda_0 \,\mathrm{tr}\,\varepsilon\delta_{ij} + 2\mu\varepsilon_{ij} - \beta p \delta_{ij}, \\ \xi &= \frac{1}{M}p + \beta\,\mathrm{tr}\,\varepsilon, \end{aligned} \tag{2.14}$$

where $\lambda_0 = \lambda_f - \beta^2 M$.

The interpretation of the coefficients λ_0, λ_f, μ, M, β in the equations (2.13) and (2.14) is the following:

9

λ_0 - is the Lame coefficient measured for an open system $(p = 0)$,

λ_f - is the Lame coefficient measured for a closed system (constant water content $\xi = 0$),

μ - classic shear modulus, as the fluid does not respond to shear forces, corresponds to a measurement for a system that is closed or open,

M - is the pressure to be exerted on the fluid to increase the fluid content a unit value, at an isovolumetric macroscopic strain of zero $(\operatorname{tr} \varepsilon = 0)$,

β - is the coefficient which quantifies the proportion due to variation in fluid content in the apparent isovolumetric macroscopic strain $\operatorname{tr} \varepsilon$ for an open system $(p = 0)$, so that it is linked not only to porosity but also to the geometry of pores where flow occurs.

Kinetic energy

Since the size of pores is small compared to the distance on which kinematic and dynamic characteristics of the motion change, volumetric kinetic energy density $\mathbf{C}$ can be restricted to the quadratic expansion

$$2\mathbf{C} = \rho \dot{u}_i \dot{u}_i + 2\rho_f \dot{u}_i \dot{w}_i + \rho_w \dot{w}_i \dot{w}_i \tag{2.15}$$

where ρ_s and ρ_f are the matrix and fluid densities respectively, ρ is the average density

$$\rho = (1 - \phi)\rho_s + \phi \rho_f \tag{2.16}$$

and ρ_w describes the coupling effect, such that

$$\rho_w = \frac{a}{\phi}\rho_f, \tag{2.17}$$

where a $(a \geqslant 1)$ is the *tortuosity* parameter which is related not only to porosity but also to the geometry of the medium where the flow occurs. Hence the equation relating a and ϕ is not unique. For example, Berryman (1980) [3] investigated the case of solid spherical particles in a fluid. For this particular case, he proposed the following relation:

$$a = \frac{1}{2}\left(\frac{1}{\phi} + 1\right). \tag{2.18}$$

Governing equations

Let $\mathbf{L}$ be the volumetric Lagrangian density defined by

$$\mathbf{L} = \mathbf{C} - \mathbf{V}. \tag{2.19}$$

The classic Euler-Lagrange equation reads:

$$\frac{\partial}{\partial t}\frac{\partial \mathbf{L}}{\partial \dot{q}_i} + \frac{\partial}{\partial x_j}\frac{\partial \mathbf{L}}{\partial q_{i,j}} - \frac{\partial \mathbf{L}}{\partial q_i} + \frac{\partial \mathbf{D}}{\partial \dot{q}_i} = 0, \tag{2.20}$$

where $\mathbf{D}$ is the dissipation pseudo-potential [9], defined as

$$\mathbf{D} = \frac{1}{K}\dot{w}_i \tag{2.21}$$

and $q_i = u_i$ or w_i.

The application of (2.20), using the expressions of $\mathbf{L}$ (2.19), $\mathbf{D}$ (2.21), $\mathbf{C}$ (2.15) and $\mathbf{V}$ (2.12), leads to the equation of motion of the form [7], [9]:

$$\begin{aligned} \sigma_{ij,j} &= \rho\ddot{u}_i + \rho_f\ddot{w}_i \\ -p_{,i} &= \rho_f\ddot{u}_i + \rho_w\ddot{w}_i + \frac{1}{K}\dot{w}_i. \end{aligned} \tag{2.22}$$

Introduction of the equations of stresses (2.13) as a function of displacements $\mathbf{u}$ and $\mathbf{U}$ in (2.22) yields the equations of motion in the form [6], [7], [9]:

$$(\lambda + 2\mu)\operatorname{grad}\operatorname{div}\mathbf{u} + Y\operatorname{grad}\operatorname{div}\mathbf{U} - \mu\operatorname{curl}\operatorname{curl}\mathbf{u} =$$

$$= \rho_{11}\ddot{\mathbf{u}} + \rho_{12}\ddot{\mathbf{U}} + b\left(\dot{\mathbf{u}} - \dot{\mathbf{U}}\right), \tag{2.23}$$

$$Y\operatorname{grad}\operatorname{div}\mathbf{u} + R\operatorname{grad}\operatorname{div}\mathbf{U} = \rho_{12}\ddot{\mathbf{u}} + \rho_{22}\ddot{\mathbf{U}} - b\left(\dot{\mathbf{u}} - \dot{\mathbf{U}}\right), \tag{2.24}$$

where it is noted:

$$\lambda = \lambda_f + M\phi(\phi - 2\beta) = \lambda_0 + M(\beta - \phi)^2, \ Y = M\phi(\beta - \phi), \ R = M\phi^2,$$

$$\rho_{11} = \rho + \phi\rho_f(a - 2), \ \rho_{12} = \phi\rho_f(1 - a), \ \rho_{22} = a\phi\rho_f, \ b = \frac{\phi^2}{K}.$$

11

λ, Y, and R are generalized poroelastic parameters which can be related to porosity ϕ, bulk modulus of the solid K_s, bulk modulus of the fluid K_f, bulk modulus of the porous drained matrix K_f, and shear modulus μ of both the drained matrix and of the composite:

$$\lambda = K_b - \frac{2}{3}\mu + \frac{K_f\left(1-\phi-\frac{K_b}{K_s}\right)^2}{\phi_{eff}}, \qquad Y = \frac{\phi K_f}{\phi_{eff}}\left(1-\phi-\frac{K_b}{K_s}\right), (2.25)$$

$$R = \frac{\phi^2 K_f}{\phi_{eff}}, \qquad \phi_{eff} = \phi + \frac{K_f}{K_s}\left(1-\phi-\frac{K_b}{K_s}\right).$$

It should be mentioned, that equations (2.23), (2.24) can be written for the limiting cases of the perfect fluid and the elastic solid by considering the following set of parameters: $\phi = \beta = a = 1$, $\lambda_f = M$ and $\mu = b = 0$ $(K \to +\infty, \eta = 0)$ for the perfect fluid, and $\phi = \beta = 0$, $a \to +\infty$ for the elastic solid [9].

2.2.2 No Dissipation Case. Slow P2 Wave

When the interaction between two phases is not well pronounced dissipation effects become negligible $(b = 0)$. For this case, introduction of the dilatational (P-waves) potential $\mathbf{\Phi} = (\Phi_1, \Phi_2)$, so that

$$\begin{pmatrix} \mathbf{u} \\ \mathbf{U} \end{pmatrix} = \text{grad}\begin{pmatrix} \Phi_1 \\ \Phi_2 \end{pmatrix} = \text{grad}\,\mathbf{\Phi} \quad \text{and} \quad \text{curl}\,\mathbf{u} = \text{curl}\,\mathbf{U} = 0 \qquad (2.26)$$

into (2.23), (2.24), leads to the following equation for the unknown potential vector:

$$\tilde{R}\nabla^2\mathbf{\Phi} - \tilde{M}\ddot{\mathbf{\Phi}} = \mathbf{0}, \qquad (2.27)$$

where $\tilde{R}$ and $\tilde{M}$ are the rigidity and mass matrix respectively:

$$\tilde{R} = \begin{pmatrix} \lambda + 2\mu & Y \\ Y & R \end{pmatrix}, \qquad \tilde{M} = \begin{pmatrix} \rho_{11} & \rho_{12} \\ \rho_{21} & \rho_{22} \end{pmatrix}. \qquad (2.28)$$

As the matrix $\tilde{R}^{-1}\tilde{M}$ is positive definite and symmetric, it has two real positive eigenvalues denoted V_{P1}^2 and V_{P2}^2, so that in the eigenvector reference system (2.27) can be written as

$$\nabla^2 \mathbf{\Phi}^* - \begin{pmatrix} \frac{1}{V_{P1}^2} & 0 \\ 0 & \frac{1}{V_{P2}^2} \end{pmatrix} \ddot{\mathbf{\Phi}}^* = \mathbf{0}, \qquad (2.29)$$

where $\mathbf{\Phi}^*$ is determined from $\mathbf{\Phi}$ by the change of coordinate system.

Two decoupled wave equations can be identified in (2.29) corresponding to the two P-wave velocities V_{P1} and V_{P2}, and to the two characteristic movements defined by the eigenvectors of $\tilde{R}^{-1}\tilde{M}$. Biot [6] showed that one of the dilatational waves corresponds to a movement in which overall and fluid displacements are in phase, and the other one to a movement in which the displacements are out of phase. The wave corresponding to the latter case is called the *slow wave* or the *wave of the second kind* (P2).

Introduction of the shear wave (S-wave) vector potential $\mathbf{\Psi} = \left(\overrightarrow{\mathbf{\Psi}}_1, \overrightarrow{\mathbf{\Psi}}_2 \right)$ so that:

$$\begin{pmatrix} \mathbf{u} \\ \mathbf{U} \end{pmatrix} = \mathrm{curl} \begin{pmatrix} \overrightarrow{\mathbf{\Psi}}_1 \\ \overrightarrow{\mathbf{\Psi}}_2 \end{pmatrix} = \mathrm{curl}\, \mathbf{\Psi} \qquad (2.30)$$

and $\mathrm{div}\, \mathbf{u} = \mathrm{div}\, \mathbf{U} = 0$ into equations (2.23), (2.24) leads to the following equations:

$$\nabla^2 \mathbf{\Psi}_1 - \frac{1}{V_S^2} \mathbf{\Psi}_1 = \mathbf{0},$$
$$\mathbf{\Psi}_2 = -\frac{\rho_{12}}{\rho_{22}} \mathbf{\Psi}_1, \qquad (2.31)$$

where velocity V_S is given by

$$V_S = \left(\frac{\mu}{\rho_{11} - \frac{\rho_{12}^2}{\rho_{22}}} \right)^{\frac{1}{2}}. \qquad (2.32)$$

Since the fluid does not respond to shear stresses in the considered model, it only influences the shear wave through inertia effects. It is obviously in phase with the overall movement as $\frac{\rho_{12}}{\rho_{22}} \leq 0$.

Experimental verification of the existence of the P2 slow wave was first obtained by Plona 1980 [37]. Results were obtained for a sample of sintered glass of porosity $\phi = 28\%$ in a water-filled tank at high frequencies (2.25MHz). Later, in 1985, slow P2 waves were observed in sea bed sediments [31].

2.2.3 Consolidation theory

The governing equations from the previous section give the most general description of the wave propagation in an isotropic porous medium adopted today. Further development of the model is usually based on more detailed consideration of the mechanical properties of the constituents, for example, including viscous effects (Biot, 1963). This leads to more complicated relations between the stress and strain tensors in Biot's equations (2.13), (2.14).

However, for certain applications such as: soil mechanics, geotechnical problems (dam problems) and some aspects of biomechanics, consolidation theory is often used. Consolidation theory is mainly concerned with the studies of time dependent settlement of porous materials. Based on Terzaghi's principle [44], [46], the governing equations for quasistatic equilibrium were first written by Biot (1941) [4].

Terzaghi's principle of effective stress [44], established primarily for 1D soil consolidation problems breaks down the total stress σ_{ij} into so-called effective stress σ_{ij}^s, which is the stress exerted on the solid skeleton, and hydrostatic stresses $p\delta_{ij}$, which is the stress due to the fluid, so that

$$\sigma_{ij} = \sigma_{ij}^s - p\delta_{ij}. \tag{2.33}$$

It can be shown [9], that Terzaghi's principle is more restrictive than Biot's theory as it assumes *a priori* that the action of the fluid can be considered as an external action exerted on the solid skeleton, and reveals the presumably additive character of the bulk moduli. This implicit assumption in Terzaghi's law leads to a partial decoupling between the fluid behavior law and that of the skeleton. The quasi-static momentum equation thus reads:

$$\frac{\partial \sigma_{ij}^s}{\partial x_j} - \frac{\partial p}{\partial x_i} = 0. \tag{2.34}$$

Biot's theory, as discussed in the previous subsection, and Terzaghi's approach are not concerned with the same field of application. Terzaghi's law is often used for the case of total saturation and frequently applied in geotechnics (flow in an earth dam, for example).

Under the assumption that the porous medium is inertia-free, the momentum equation ($\sigma_{ij,j} = 0$) becomes:

$$(\lambda + 2\mu)\operatorname{grad}\operatorname{div}\mathbf{u} - \mu\operatorname{curl}\operatorname{curl}\mathbf{u} - \operatorname{grad} p = 0. \tag{2.35}$$

Storage equation

Another equation is required in order to close the system. Differentiating equation (2.14) with respect to time and using the steady-state Darcy's law (2.4) one can obtain

$$\frac{\partial}{\partial t}\operatorname{div}\mathbf{u} = -\frac{1}{M}\frac{\partial p}{\partial t} + K\operatorname{div}\operatorname{grad}p, \tag{2.36}$$

where $M = \phi\gamma$, γ represents the compressibility of the saturating fluid [47] (for example, due to dissolved gas bubbles).

Equation (2.36) is a *storage equation*. It is one of the most important equations of consolidation theory. A rigorous derivation of (2.36) based on principles of conservation of mass can be found in [47].

The storage equation may be written in the form:

$$\frac{\partial}{\partial t}\operatorname{div}\mathbf{u} = -\frac{1}{M}\frac{\partial p}{\partial t} - \frac{\partial}{\partial t}\operatorname{div}\mathbf{w} \tag{2.37}$$

and admits a simple heuristic interpretation: compression of the porous medium element consists of the compression of the pore fluid plus the amount of fluid expelled from the element by flow.

Undrained deformations

The equations can be further simplified for problems concerned with a rapid loading of a compressible poroelastic material. In this case, comparative fluid motion in the elementary volume is expected to be negligibly small, so that consolidation process can be simplified in the following way [47]: integrating (2.37) over a short period of time $\triangle t$ one obtains

$$\triangle\operatorname{div}\mathbf{u} = -\frac{1}{M}\triangle p - \triangle\operatorname{div}\mathbf{w}. \tag{2.38}$$

When the permeability is small, the term $\triangle\operatorname{div}\mathbf{w}$ representing the net outward flow over time interval $\triangle t$ may be neglected. If the volume strain and the pore pressure are considered to be incremental values with respect to their initial values one can write

$$\operatorname{div} \mathbf{u} = -\frac{1}{M}p. \tag{2.39}$$

So that, eliminating the pore pressure from the momentum equation one can get

$$(\lambda^* + 2\mu)\operatorname{grad}\operatorname{div}\mathbf{u} - \mu\operatorname{curl}\operatorname{curl}\mathbf{u} = 0, \tag{2.40}$$

where $\lambda^* = \lambda_0 + M$.

This equation is completely analogous to the momentum equation of static equilibrium for an elastic solid material, except that the Lame coefficient λ_0 is replaced by λ^*.

Chapter 3

Basic 1D diffusion solutions for semi-infinite domain

The governing equations of consolidation theory are represented by a momentum equation (2.35) and storage equation (2.36), so that for the one dimensional (henceforth 1D) case we have

$$(\lambda + 2\mu) \frac{\partial^2 u(x,t)}{\partial x^2} - \frac{\partial p(x,t)}{\partial x} = 0, \tag{3.1}$$

$$\frac{\partial}{\partial x} \left(\frac{\partial u(x,t)}{\partial t} - K \frac{\partial p(x,t)}{\partial x} \right) = -\frac{1}{M} \frac{\partial p}{\partial t}. \tag{3.2}$$

The system of equations (3.1), (3.2) can often be reduced to the diffusion equation either for the unknown solid phase displacement u or for the unknown pressure p.

The one dimensional steady-state Darcy law (2.4) reads:

$$\frac{\partial w(x,t)}{\partial t} = -K \frac{\partial p(x,t)}{\partial x}. \tag{3.3}$$

This equation can be used to determine the fluid phase displacements U from known u and p, using the definition of the filtration velocity and applying corresponding boundary conditions. In other words, equations (3.1), (3.2) are prognostic equations which determine u and p, and afterwards the solution for the filtration velocity $\dot{w}$ can be obtained from the diagnostic equations (3.3).

The diffusion equation has many simple analytical solutions for a semi-infinite domain, while in the case of finite length domains, application of various numerical

methods is preferred. In the present chapter the focus is on the simple analytical solutions for a semi infinite domain, so that questions regarding reflection from the boundary will not be considered.

The parameter M (dimension of pressure) in the storage equation (3.2) corresponds to the compressibility property of the porous medium, so that setting $M \gg 1$ implies incompressibility of porous medium. In this case, the storage equation (2.37) reduces to

$$\frac{\partial}{\partial t} \operatorname{div} \mathbf{u} = -\frac{\partial}{\partial t} \operatorname{div} \mathbf{w} \tag{3.4}$$

and using the definition of the filtration velocity (2.2) one can get

$$\operatorname{div} \left[(1 - \phi) \, \dot{\mathbf{u}} + \phi \dot{\mathbf{U}} \right] = 0. \tag{3.5}$$

This equation has a simple physical interpretation: an elementary volume of the porous material under the assumption of large M is incompressible. In this case the variation of the isovolumetric strain is equal to the variation of fluid content in the element.

Two main types of problems can be considered, depending on whether we have a fixed water content in the medium (*undrained deformations*) or variation of fluid content (*drained deformations*).

As the consolidation theory concerns mainly the problems of time dependent settlements of porous materials subjected to the certain types of loading, choices for the boundary conditions follow from physical interpretations. In this regard, it is important to emphasize that by definition, the effective stress σ_{ij}^s is not the average stress in the grains, but a measure of the forces transmitted from particle to particle at the contact points.

For example, consider porous material in contact with water, so that some external pressure $P_0(t)$ is exerted on the boundary. In this case we have

$$\sigma_x^s(0, t) = 0, \qquad p(0, t) = P_0(t), \tag{3.6}$$

so that the total stress at the boundary, by definition, is $\sigma_{ij}(0, t) = -P_0(t)\delta_{ij}$. Then the problem is to determine the settlement and the pore pressure distribution. A more general formulation can be obtained for the case of a thick permeable membrane located at the interface:

$$\sigma_x^s(0,t) = -Q(t), \qquad p(0,t) = P_0(t). \tag{3.7}$$

Now, the effective stress is not zero at the boundary, but is described by the function $Q(t)$ which is a measure of the forces transmitted by the membrane to the grains. We shall refer to this problem as the *liquid piston problem*.

In the particular case of the *creep problem* we may, for example, consider a loading with a perfectly permeable membrane so that

$$\sigma_x^s(0,t) = -Q(t), \qquad p(0,t) = 0. \tag{3.8}$$

Again, the problem is to determine the time dependent settlement as well as the pore pressure distribution in the interior of the porous material.

When the settlement of the boundary is prescribed, one can determine the settlement in the interior as well as the pore pressure. In this case (referred to as the *permeable piston problem*) boundary conditions will be given in the following way:

$$u(0,t) = u_0(t), \qquad p(0,t) = 0. \tag{3.9}$$

In the following chapter, solutions of the above mentioned problems will be obtained for the case of zero initial conditions, with the boundary conditions prescribed using the Dirac function $\delta(t)$ or Heaviside step function $H(t)$ time dependence to represent transient loads. Because of the linearity of the governing equations it is possible to represent a solution for an arbitrary loading function $F(t)$ as a convolution with the above obtained solutions (Duhamel's integral). In practice, elementary solutions obtained below can be convolved with the functions representing some smooth impulsively started forcing in order to get physically meaningful solutions. For example, for the general solid phase displacement $u^F(x,t)$ we have

$$u^F(x,t) = \dot{F} * u = u_0 \int_0^t \dot{F}(\tau)u^H(x,t-\tau)d\tau = u_0 \int_0^t F(\tau)u^\delta(x,t-\tau)d\tau. \tag{3.10}$$

where $u^H(x,t)$, $u^\delta(x,t)$ are the solutions of the problem, obtained for the boundary conditions $u(0,t) = u_0 H(t)$ and $u(0,t) = u_0\delta(t)$ respectively.

3.1 Permeable piston problem

3.1.1 Incompressible medium

A saturated porous material occupying a 1D semi-infinite domain $x \geq 0$ is considered. The momentum equation (3.1), reads:

$$(\lambda + 2\mu) \frac{\partial^2 u(x,t)}{\partial x^2} - \frac{\partial p(x,t)}{\partial x} = 0. \tag{3.11}$$

The 1D storage equation, assuming the incompressibility condition $M >> 1$, simplifies to

$$\frac{\partial}{\partial x} \left(\frac{\partial u(x,t)}{\partial t} - K \frac{\partial p(x,t)}{\partial x} \right) = 0. \tag{3.12}$$

The steady-state Darcy's law reads:

$$\frac{\partial w(x,t)}{\partial t} = -K \frac{\partial p(x,t)}{\partial x}. \tag{3.13}$$

Initial conditions for the fluid and solid phase displacements, as well as for the pressure, are set to zero:

$$u(x,0) = U(x,0) = p(x,0) = 0. \tag{3.14}$$

The following boundary conditions are prescribed at $x = 0$:

$$u(0,t) = u_0 H(t), \tag{3.15}$$

$$p(0,t) = 0, \tag{3.16}$$

so that, in this idealized problem instantaneous compression of the solid matrix is considered, while pressure at the boundary is zero. Physical considerations imply that due to the dissipation resulting from the relative fluid/solid interactions, both solid u and fluid U phase displacements must vanish at infinity:

$$\lim_{x \to \infty} u(x,t) = \lim_{x \to \infty} U(x,t) = 0. \tag{3.17}$$
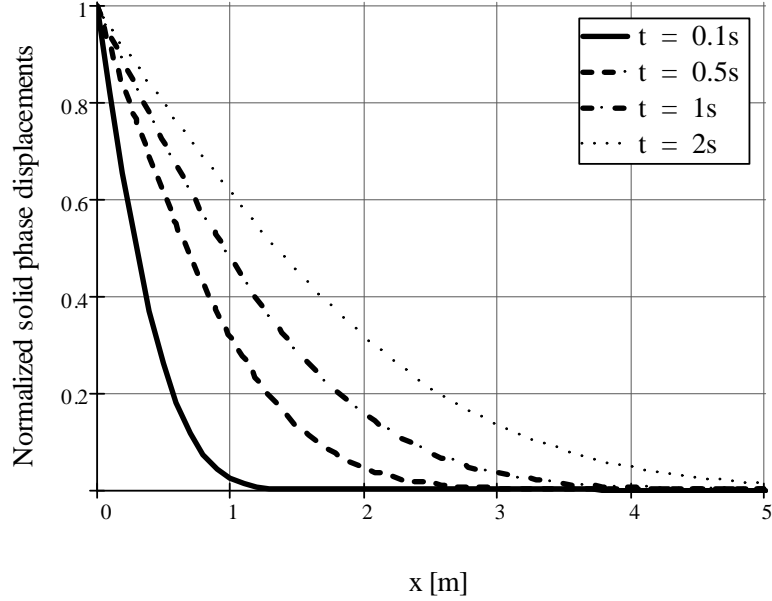
Figure 3.1: Normalized solid phase displacements $\frac{u(x,t)}{u_0}$, evaluated for the consecutive time steps $(a = 1)$

From (3.17) it can be also inferred that the filtration velocity vanishes along with the pressure gradient: $\lim_{x\to\infty} \dot{w}(x,t) = 0$, so that $\lim_{x\to\infty} \frac{\partial p(x,t)}{\partial x} = 0$, as follows from (3.13).

The far field conditions (3.17) greatly simplify the problem, reducing the order of the system; equations (3.1) and (3.12) can now be written the following way:

$$(\lambda + 2\mu)\frac{\partial u(x,t)}{\partial x} - p(x,t) = f(t), \tag{3.18}$$

$$\frac{\partial u(x,t)}{\partial t} - K\frac{\partial p(x,t)}{\partial x} = 0, \tag{3.19}$$

where $f(t)$ is an arbitrary function of time to be defined from the boundary conditions.

Equations (3.18) and (3.19) can be reduced to the heat equation:

$$u_{xx}(x,t) = a \cdot u_t(x,t), \tag{3.20}$$

21

where $a = \frac{1}{(\lambda+2\mu)K} = \frac{\eta}{(\lambda+2\mu)k}$ is the consolidation coefficient (for example, in the case of water saturated sandstone: Lame coefficients $\lambda, \mu \approx 10^8 - 10^9 \frac{kg}{ms^2}$, water dynamic viscosity $\eta = 1.78 \cdot 10^{-3} \frac{kg}{ms}$, permeability $k \approx 10^{-16} - 10^{-13} m^2$; in this particular case $a \approx 1 - 10^5 \frac{s}{m}$).

Applying the Laplace transform to the problem (3.20), (3.15) one can get the following solution for the problem in Laplace space:

$$
\begin{aligned}
u(x,s) &= A(s)e^{-x\sqrt{as}} + B(s)e^{x\sqrt{as}}, \\
u(0,s) &= \frac{u_0}{s}.
\end{aligned}
\tag{3.21}
$$

According to the far field conditions (3.17), the coefficient $B(s)$ has to be zero, and we only take into account "waves" propagating from the origin to infinity. The solution for the solid phase displacement can thus be written as

$$
u(x,s) = \frac{u_0}{s}e^{-x\sqrt{as}},
\tag{3.22}
$$

so that the inverse Laplace transform gives

$$
u(x,t) = u_0 \operatorname{erfc}\left(\frac{x\sqrt{a}}{2\sqrt{t}}\right),
\tag{3.23}
$$

where erfc is the complementary error function

$$
\operatorname{erfc}(x) = \frac{2}{\sqrt{\pi}} \int_x^\infty e^{-t^2} dt = 1 - \operatorname{erf}(x) = 1 - \frac{2}{\sqrt{\pi}} \int_0^x e^{-t^2} dt.
$$

Above, the well known expression for the Laplace transform pair was used [21]:

$$
\frac{1}{s}e^{-k\sqrt{s}} \doteqdot \operatorname{erfc}\left(\frac{k}{2\sqrt{t}}\right) \qquad (k > 0,\, t > 0).
$$

Now, pressure can be determined from (3.18) and (3.16):

$$
p(x,t) = \frac{u_0}{K} \frac{\left(1 - e^{-\frac{ax^2}{4t}}\right)}{\sqrt{\pi a t}}
\tag{3.24}
$$

22
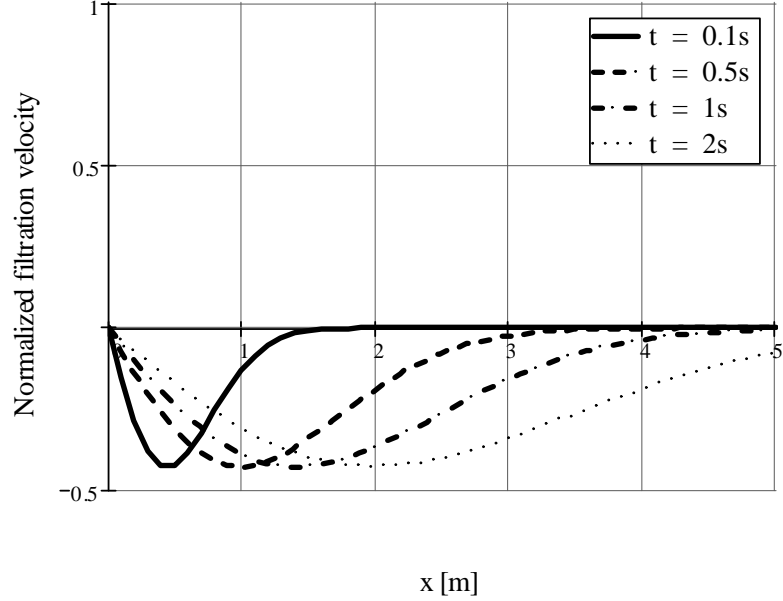
Figure 3.2: Filtration velocity diffusion ($a = 1$)

and, using (3.13), it is possible to obtain the expression for the filtration velocity $W(x,t)$:

$$W(x,t) = \dot{w}(x,t) = -\frac{u_0 x \sqrt{a}}{2t\sqrt{\pi t}} e^{-\frac{ax^2}{4t}}. \tag{3.25}$$

The solution indeed satisfies all the requirements, as can be checked by direct substitution into the governing equations and boundary conditions. Using the Laplace transform method, the initial conditions were satisfied automatically.

Non-dimensional quantities can be introduced in the following way:

$$q = \frac{x\sqrt{a}}{\sqrt{t}}, \quad \tilde{u} = \frac{u}{u_0}, \quad \tilde{p} = \frac{K\sqrt{\pi a t}}{u_0} p, \quad \tilde{W} = \frac{t\sqrt{\pi}}{u_0} W, \tag{3.26}$$

so that in non-dimensional notation, omitting tildes, we have

$$u(q) = \operatorname{erfc}\left(\frac{q}{2}\right), \quad p(q) = 1 - e^{-\frac{q^2}{4}}, \quad W = -\frac{q}{2} e^{-\frac{q^2}{4}}. \tag{3.27}$$

Solution of a more general problem (arbitrary piston trajectory $F(t)$) can be

23
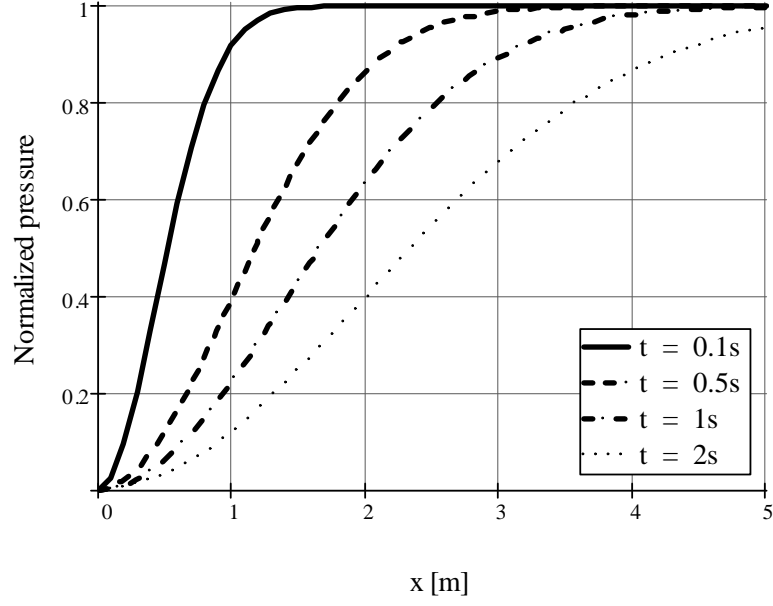
Figure 3.3: Pore pressure diffusion ($a = 1$)

written down based on the solution with a Heaviside loading, for example, for the solid phase displacement u^F we have

$$u^F(x,t) = \dot{F} * u = u_0 \int_0^t \dot{F}(\tau) \operatorname{erfc}\left(\frac{x\sqrt{a}}{2\sqrt{t-\tau}}\right) d\tau. \tag{3.28}$$

As can be noted from (3.24), (3.25), both pore pressure and filtration velocity attenuate as $\frac{1}{t^{3/2}}$ with respect to time. Figures 3.1, 3.2, 3.3 illustrate normalized solid phase displacements, filtration velocity diffusion and pressure diffusion respectively.

3.1.2 Compressible medium

We now consider a similar, but more general problem for the compressible medium. In this case, instead of making the assumption of large M (3.12), the 1D balance equation will be used in its general form (3.2):

$$\frac{\partial}{\partial x}\left(\frac{\partial u}{\partial t} - K\frac{\partial p}{\partial x}\right) = -\frac{1}{M}\frac{\partial p}{\partial t}. \tag{3.29}$$

24

The parameter M reflects the compressibility property of the saturating fluid and can be expressed in terms of the porosity ϕ and compressibility γ (for pure water $\gamma = 0.5 \cdot 10^{-9} \frac{m^2}{kN}$):

$$M = \frac{1}{\phi\gamma}. \tag{3.30}$$

For the governing equations (3.1), (3.2) and (3.13) zero initial conditions (3.14) are prescribed. Again, we assume zero far field conditions (3.17). Like before, boundary conditions (3.15) and (3.16) are used to describe an instantaneous loading (permeable piston).

In this case, differentiating the momentum equation (3.1) with respect to time t, and the storage equation (3.2) with respect to x one can obtain

$$(\lambda + 2\mu)\, u_{xxt} = p_{xt}, \tag{3.31}$$

$$\frac{\partial^2}{\partial x^2}\left(u_t - \frac{1}{a}u_{xx}\right) = -\frac{1}{M}p_{xt} = -\frac{\lambda + 2\mu}{M}u_{xxt}. \tag{3.32}$$

Integration with respect to x twice and application of the far field conditions reduces the latter equation to the following diffusion equation:

$$u_{xx}(x,t) = a(1 + \tilde{M}) \cdot u_t(x,t), \tag{3.33}$$

where $\tilde{M} = \frac{\lambda + 2\mu}{M}$. Note that since $\lambda + 2\mu = O(10^9)$ we have that $\tilde{M}$ is order 1. Henceforth tildes over M are omitted.

The solution for the solid phase displacements can be obtained in the form

$$u(x,t) = u_0 \operatorname{erfc}\left(\frac{x\sqrt{a(1+M)}}{2\sqrt{t}}\right). \tag{3.34}$$

The pressure field (using equation (3.31) and (3.16)) becomes

$$p(x,t) = \frac{u_0\sqrt{1+M}}{K}\frac{\left(1 - e^{-a(1+M)\frac{x^2}{4t}}\right)}{\sqrt{\pi a t}}. \tag{3.35}$$

25
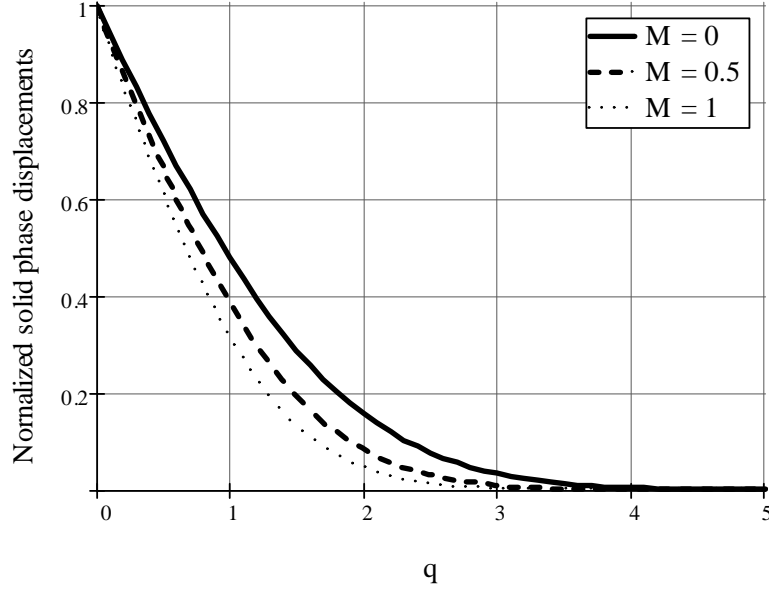
Figure 3.4: Normalized solid phase displacements ($a = 1$, $M = 0$ (incompressible), $M = 0.5$, $M = 1$)

The expression for the filtration velocity $W(x,t)$ can be found to be

$$W(x,t) = \dot{w}(x,t) = -\frac{u_0\sqrt{1 + M}x\sqrt{a}}{2t\sqrt{\pi t}}e^{-a(1+M)\frac{x^2}{4t}}. \tag{3.36}$$

The solution for the incompressible medium, obtained in the previous section is a benchmark solution for the compressible medium: setting $M = 0$ we recover the incompressible case.

Figures 3.4, 3.5 represent normalized (according to (3.26)) solid phase displacements and pressure for incompressible ($M = 0$, solid lines) and compressible cases ($M = 0.5$, $M = 1$). Comparison of the solutions for the compressible and incompressible case shows the following: when the solid matrix is subjected to a compression, the pore pressure jump is larger for the compressible pore fluid, compared to the incompressible case (see Figure 3.5). At the same time the incompressible case shows more intense solid phase motion (see Figure 3.4).
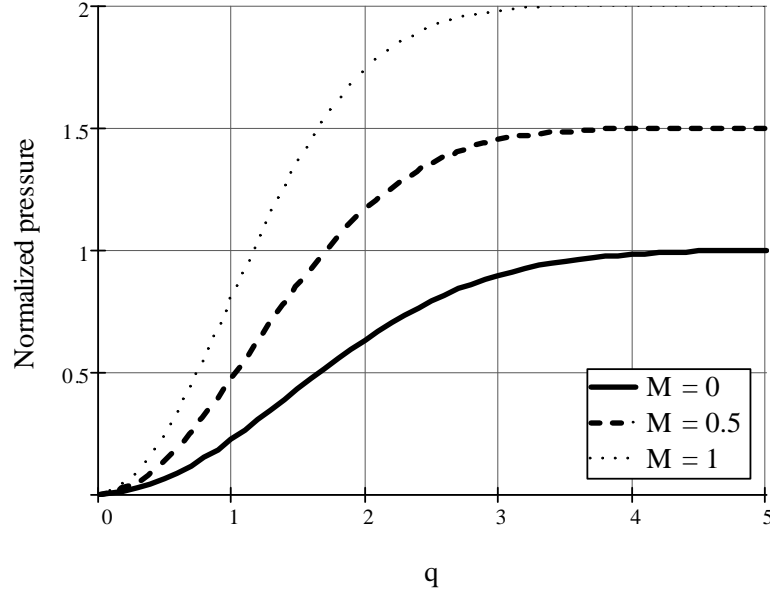
Figure 3.5: Normalized pressure ($a = 1$, $M = 0$ (incompressible), $M = 0.5$, $M = 1$)

3.2 Creep problem

Assume again that the porous material occupies a semi infinite domain $x \geq 0$. Initially, the material is at rest, but at $t = 0$ there is a certain pressure exerted on the solid matrix only (for example, consider a perfectly permeable membrane). This is a case of a creep problem with an effective stress specified. Unlike the previous case, the trajectory of the piston is unknown, and we investigate how external traction influences the dynamics of the porous material (pore pressure, settlement, filtration).

An effective stress can be prescribed at the boundary in the following way:

$$\text{at} \ \ x = 0: \qquad \sigma_x^s(0, t) = -QH(t), \qquad p(0, t) = \ 0, \tag{3.37}$$

so that we have an instantaneous pressure jump of magnitude Q.

The above considerations can be used to reduce the system of governing equations to the diffusion equation from the previous subsection:

$$u_{xx}(x, t) = \tilde{a} \cdot u_t(x, t), \tag{3.38}$$

27

where $\tilde{a} = a(1 + \tilde{M})$.

The solution in Laplace space can be written down as

$$u(x, s) = A(s)e^{-x\sqrt{\tilde{a}s}}, \tag{3.39}$$

so that

$$u_x(x, s) = -\sqrt{\tilde{a}s}A(s)e^{-x\sqrt{\tilde{a}s}}, \tag{3.40}$$

Now in order to determine $A(s)$, the expression for the effective stress can be used. In the Laplace space it reads

$$\sigma_x^s(0, s) = (\lambda + 2\mu)\, u_x(0, s) = -\frac{Q}{s} \tag{3.41}$$

and the expression for $A(s)$ becomes

$$A(s) = \frac{Q}{(\lambda + 2\mu)}\frac{1}{s\sqrt{\tilde{a}s}}. \tag{3.42}$$

Now, using the well known expression for the Laplace transform pair [21]:

$$\frac{1}{s\sqrt{s}}e^{-k\sqrt{s}} \doteq 2\sqrt{\frac{t}{\pi}}e^{-\frac{k^2}{4t}} - k\operatorname{erfc}\left(\frac{k}{2\sqrt{t}}\right) \qquad (k \geq 0,\, t > 0) \tag{3.43}$$

the expression for solid phase displacements in physical space becomes

$$u(x, t) = \frac{Q}{\sqrt{\tilde{a}}(\lambda + 2\mu)}\left(2\sqrt{\frac{t}{\pi}}e^{-\frac{x^2\tilde{a}}{4t}} - x\sqrt{\tilde{a}}\operatorname{erfc}\left(\frac{x\sqrt{\tilde{a}}}{2\sqrt{t}}\right)\right). \tag{3.44}$$

The trajectory of the boundary can be found as

$$u(0, t) = \frac{2Q\sqrt{t}}{\sqrt{\pi\tilde{a}}(\lambda + 2\mu)}. \tag{3.45}$$

Thus, the velocity of the piston attenuates as $\frac{1}{\sqrt{t}}$ and is unbounded as $t \to 0^+$.

The effective stress is given by

$$\sigma_x^s(x, t) = (\lambda + 2\mu)\, u_x(x, t) = -Q\operatorname{erfc}\left(\frac{x\sqrt{\tilde{a}}}{2\sqrt{t}}\right), \tag{3.46}$$

28

so that taking into account (3.18), an expression for the pressure satisfying the boundary condition (3.16) can be found as

$$p(x,t) = Q\left[1 - \operatorname{erfc}\left(\frac{x\sqrt{\tilde{a}}}{2\sqrt{t}}\right)\right] = Q\operatorname{erf}\left(\frac{x\sqrt{\tilde{a}}}{2\sqrt{t}}\right). \tag{3.47}$$

Thus, a solid matrix loading causes a pressure jump, with the initial magnitude equal to the pressure exerted on the solid matrix. Subsequently, the pressure diffuses due to fluid motion and returns to its initial value. Filtration velocity can be recovered from (3.13).

3.3   Liquid piston problem

Assume that the porous material occupies a semi-infinite domain $x \geq 0$ so that it has a common boundary with an area occupied by fluid ($-l \leq x \leq 0$ or $x \leq 0$). If we consider a membrane on the interface such that pressure perturbation in the surrounding fluid exerts some external pressure on porous material, both the solid matrix and fluid phase will be subjected to a certain traction.

Boundary conditions can be expressed in the following way:

$$\text{at } x = 0: \qquad \sigma_x^s(0,t) = -Q\delta(t), \qquad p(0,t) = P\delta(t), \tag{3.48}$$

so that the quantities Q and P are introduced to describe the distribution of the traction between the matrix and pore pressure (dimension of momentum per unit area).

The above considerations can be used to reduce the system of governing equations to the diffusion equation from the previous subsection:

$$u_{xx}(x,t) = \tilde{a} \cdot u_t(x,t), \tag{3.49}$$

where $\tilde{a} = a(1 + \tilde{M})$.

The solution in Laplace space can be written down as

$$u(x,s) = A(s)e^{-x\sqrt{\tilde{a}s}}, \tag{3.50}$$

so that

29

$$u_x(x, s) = -\sqrt{\tilde{a}s}A(s)e^{-x\sqrt{\tilde{a}s}}. \tag{3.51}$$

Now in order to determine $A(s)$, the expression for the effective stress can be used. In the Laplace space we have

$$\sigma_x^s(0, s) = (\lambda + 2\mu)\, u_x(0, s) = -Q \tag{3.52}$$

and the expression for $A(s)$ becomes

$$A(s) = \frac{Q}{\sqrt{\tilde{a}s}(\lambda + 2\mu)}. \tag{3.53}$$

Again, using the well known expression for the Laplace transform pair [21]:

$$\frac{1}{\sqrt{s}}e^{-k\sqrt{s}} \doteq \frac{1}{\sqrt{\pi t}}e^{-\frac{k^2}{4t}} \qquad (k \geq 0,\, t > 0) \tag{3.54}$$

the expression for solid phase displacements in physical space becomes

$$u(x, t) = \frac{Q}{\sqrt{\tilde{a}}(\lambda + 2\mu)} \frac{1}{\sqrt{\pi t}}e^{-\frac{x^2\tilde{a}}{4t}}. \tag{3.55}$$

The effective stress is given by

$$\sigma_x^s(x, t) = (\lambda + 2\mu)\, u_x(x, t) = -\frac{Qx\sqrt{\tilde{a}}}{2t\sqrt{\pi t}}e^{-\frac{x^2\tilde{a}}{4t}}, \tag{3.56}$$

so that taking into account the limit representation of the Dirac function which follows from the boundary condition (3.48) and (3.56):

$$\delta(t) = \lim_{x \to 0}\left(\frac{x}{2t\sqrt{\pi t}}e^{-\frac{x^2}{4t}}\right), \tag{3.57}$$

an expression for the pressure satisfying boundary condition (3.48) can be found as

$$p(x, t) = -Q\frac{x\sqrt{\tilde{a}}}{2t\sqrt{\pi t}}e^{-\frac{x^2\tilde{a}}{4t}} + (P + Q)\,\delta(t). \tag{3.58}$$

3.4 Final remarks

Consolidation theory, established by Terzaghi [44] and Biot [4], is the simplest mathematical model to describe basic processes in a binary (two phase) medium. Thus, the application of the theory is limited to a certain class of problems, for example, long term settlement problems in geomechanics. The range of applicability of a particular set of parameters is also restricted to a limited class of problems. Diffusion type solutions, such as those derived in the previous sections, assume an infinite speed of signal propagation in the porous medium and in certain situations this is obviously unphysical. Still consolidation theory has found broad applications both in geomechanics and biomechanics.

In order to study wave propagation in a porous medium, we must account for inertia terms in the governing equations. This was originally done by Biot [6], and the next chapter is dedicated to several boundary value problems in a porous half-space governed by Biot's theory.

Chapter 4

Wave propagation

Boundary value problems for a poroelastic half-space in the framework of Biot's theory were considered, for example, in [23], [14], [36], [45], [41], [29], [19], [33], [28]. Generally speaking, two main types of problems arise: so called steady state problems, when harmonic time dependence is assumed for the imposed tractions (and consequently for the stress and displacement fields), and the problems of the transient response when impulsive tractions are applied. The latter class of problems is much more complicated, however, the value of the results obtained can hardly be overestimated for many engineering applications (for example seismoacoustic exploration and non-destructive testing).

This chapter is organized in the following way: first, a detailed introduction of the Helmholtz potentials is discussed, then, based on the expressions obtained, the exact Fourier - Laplace solution for Lamb's problem is derived for a medium with a free pressure at the boundary, subjected to a normal load (the permeable piston problem). Based on the general solution, two cases are investigated thoroughly: steady state line traction and impulsive line traction. For the steady state case, an exact Green's function is presented, as well as the solution for a distributed traction. For the impulsive traction, a simplified model is considered (non-dissipative fully saturated medium) and an analytic solution is derived using the Cagniard de Hoop inversion technique. Finally, an analysis of the secular equation of the surface waves (Rayleigh waves) is presented for both dissipative and non dissipative media.

Numerical results are presented for two sets of poroelastic parameters (see Appendix F) - Fatt's model and water saturated Berea sandstone.

4.1 Introduction of the potentials

Consider Biot's set of equations (2.23), (2.24) [9], [7]:

$$(\lambda + \mu)\operatorname{grad}\operatorname{div}\mathbf{u} + \mu\nabla^2\mathbf{u} + Y\operatorname{grad}\operatorname{div}\mathbf{U} = \rho_{11}\ddot{\mathbf{u}} + \rho_{12}\ddot{\mathbf{U}} + b\left(\dot{\mathbf{u}} - \dot{\mathbf{U}}\right),$$

$$Y\operatorname{grad}\operatorname{div}\mathbf{u} + R\operatorname{grad}\operatorname{div}\mathbf{U} = \rho_{12}\ddot{\mathbf{u}} + \rho_{22}\ddot{\mathbf{U}} - b\left(\dot{\mathbf{u}} - \dot{\mathbf{U}}\right). \tag{4.1}$$

Expansion of the displacement field into irrotational and solenoidal parts yields

$$\begin{aligned}
\mathbf{u} &= \operatorname{grad}\Phi_1 + \operatorname{curl}\overrightarrow{\Psi}_1, & \operatorname{curl}\Phi_1 = 0, \ \operatorname{div}\overrightarrow{\Psi}_1 = 0, \\
\mathbf{U} &= \operatorname{grad}\Phi_2 + \operatorname{curl}\overrightarrow{\Psi}_2, & \operatorname{curl}\Phi_2 = 0, \ \operatorname{div}\overrightarrow{\Psi}_2 = 0
\end{aligned} \tag{4.2}$$

and results in the following scalar and vector set of equations in Laplace space:

$$\begin{aligned}
(\lambda + 2\mu)\nabla^2\Phi_1 + Y\nabla^2\Phi_2 &= \rho_{11}s^2\Phi_1 + \rho_{12}s^2\Phi_2 + bs\left(\Phi_1 - \Phi_2\right), \\
Y\nabla^2\Phi_1 + R\nabla^2\Phi_2 &= \rho_{12}s^2\Phi_1 + \rho_{22}s^2\Phi_2 - bs\left(\Phi_1 - \Phi_2\right), \\
\mu\nabla^2\overrightarrow{\Psi}_1 &= \rho_{11}s^2\overrightarrow{\Psi}_1 + \rho_{12}s^2\overrightarrow{\Psi}_2 + bs\left(\overrightarrow{\Psi}_1 - \overrightarrow{\Psi}_2\right), \\
0 &= \rho_{12}s^2\overrightarrow{\Psi}_1 + \rho_{22}s^2\overrightarrow{\Psi}_2 - bs\left(\overrightarrow{\Psi}_1 - \overrightarrow{\Psi}_2\right).
\end{aligned} \tag{4.3}$$

The first two equations may be rewritten in the matrix form:

$$\nabla^2\begin{pmatrix}\Phi_1 \\ \Phi_2\end{pmatrix} = \tilde{R}^{-1}\tilde{N}\begin{pmatrix}\Phi_1 \\ \Phi_2\end{pmatrix}, \tag{4.4}$$

where $\tilde{R}^{-1}$ is the inverse of the rigidity matrix:

$$\tilde{R} = \begin{pmatrix}\lambda + 2\mu & Y \\ Y & R\end{pmatrix}, \qquad \tilde{R}^{-1} = \frac{1}{\det\tilde{R}}\begin{pmatrix}R & -Y \\ -Y & \lambda + 2\mu\end{pmatrix}$$

and the components of $\tilde{N}$ are given by

$$\tilde{N} = s^2\begin{pmatrix}\rho_{11} + b/s & \rho_{12} - b/s \\ \rho_{12} - b/s & \rho_{22} + b/s\end{pmatrix}.$$

So that

$$\tilde{R}^{-1}\tilde{N} = \frac{s^2}{(\lambda + 2\mu)\, R - Y^2} \begin{pmatrix} a_{11} & a_{12} \\ a_{21} & a_{22} \end{pmatrix},$$

where

$$
\begin{aligned}
a_{11} &= R(\rho_{11} + b/s) - Y(\rho_{12} - b/s), \\
a_{12} &= R(\rho_{12} - b/s) - Y(\rho_{22} + b/s), \\
a_{21} &= -Y(\rho_{11} + b/s) + (\lambda + 2\mu)(\rho_{12} - b/s), \\
a_{22} &= -Y(\rho_{12} - b/s) + (\lambda + 2\mu)(\rho_{22} + b/s).
\end{aligned}
$$

Introduction of nondimensional quantities in accordance with [6]:

$$
\begin{aligned}
\gamma_{11} &= \rho_{11}/\rho,\ \gamma_{12} = \rho_{12}/\rho,\ \gamma_{22} = \rho_{22}/\rho,\ \rho = \rho_{11} + \rho_{22} + 2\rho_{12},\ c^2 = H/\rho, \quad (4.5) \\
q_{11} &= (\lambda + 2\mu)/H,\ q_{12} = Y/H,\ q_{22} = R/H,\ H = \lambda + 2\mu + R + 2Y
\end{aligned}
$$

leads to the following form of the matrix $\tilde{R}^{-1}\tilde{N}$:

$$\tilde{R}^{-1}\tilde{N} = \frac{s^2 \rho H}{(\lambda + 2\mu)\, R - Y^2} \begin{pmatrix} \tilde{a}_{11} & \tilde{a}_{12} \\ \tilde{a}_{21} & \tilde{a}_{22} \end{pmatrix},$$

where

$$
\begin{aligned}
\tilde{a}_{11} &= q_{22}(\gamma_{11} + b/\rho s) - q_{12}(\gamma_{12} - b/\rho s), \\
\tilde{a}_{12} &= q_{22}(\gamma_{12} - b/\rho s) - q_{12}(\gamma_{22} + b/\rho s), \\
\tilde{a}_{21} &= -q_{12}(\gamma_{11} + b/\rho s) + q_{11}(\gamma_{12} - b/\rho s), \\
\tilde{a}_{22} &= -q_{12}(\gamma_{12} - b/\rho s) + q_{11}(\gamma_{22} + b/\rho s). \quad (4.6)
\end{aligned}
$$

Denoting the eigenvalues of the matrix $\tilde{R}^{-1}\tilde{N}$ as z_1 and z_2, such that

$$z_{1,2} = \frac{s^2 \rho H}{(\lambda + 2\mu)\, R - Y^2}\, \tilde{z}_{1,2} = \frac{s^2 \rho}{H(q_{11} q_{22} - q_{12}^2)}\, \tilde{z}_{1,2},$$

we arrive at the following characteristic equation:

$$\tilde{z}^2 - (q_{11}\gamma_{22} + q_{22}\gamma_{11} - 2q_{12}\gamma_{12} + b/\rho s)\tilde{z} + (q_{11}q_{22} - q_{12}^2)(\gamma_{11}\gamma_{22} - \gamma_{12}^2 + b/\rho s) = 0,$$

which can be rewritten for non-dimensional $\bar{z}$ in the following way:

$$(q_{11}q_{22} - q_{12}^2)\bar{z}^2 - (q_{11}\gamma_{22} + q_{22}\gamma_{11} - 2q_{12}\gamma_{12} + b/\rho s)\bar{z} + (\gamma_{11}\gamma_{22} - \gamma_{12}^2 + b/\rho s) = 0, \quad (4.7)$$

where $\tilde{z}_{1,2} = \frac{s^2\rho}{H}\bar{z}$.

The above equation first appeared in the fundamental work by Biot [6] as a dispersion relation for the longtitudal waves and was used therein for the detailed numerical analysis of the P1, P2 - waves' dispersion characteristics. While Biot provided a numerical analysis in his work, Geerstma and Smith [20] arrived at the same conclusions suggesting an approximate solution of the frequency equation (4.7). They noticed that for most porous rock materials certain regularity for the coefficients of equation (4.7) holds.

Dilatational waves (P-waves)

The equation (4.4) in an eigenvector reference system decouples into two wave equations:

$$\nabla^2\Phi_1^* = \frac{s^2\bar{z}_1}{c^2}\Phi_1^*, \quad \nabla^2\Phi_2^* = \frac{s^2\bar{z}_2}{c^2}\Phi_2^*. \quad (4.8)$$

The above equations describe P1- and P2-wave behavior respectively, with phase velocities given by

$$V_{P_1} = \frac{c}{\sqrt{\bar{z}_1}}, \quad V_{P_2} = \frac{c}{\sqrt{\bar{z}_2}}.$$

The P1-wave corresponds to the case when solid and liquid displacements are in phase, while the P2-wave describes out of phase motion (formally - filtration) [6], [9]. Moreover, waves of the first kind propagate faster and attenuate slower compared to the wave of the second kind.

The connection between the reference systems is given by the eigenvector matrix $\tilde{V}$:

$$\begin{pmatrix} \Phi_1 \\ \Phi_2 \end{pmatrix} = \tilde{V}\begin{pmatrix} \Phi_1^* \\ \Phi_2^* \end{pmatrix}, \quad \tilde{V} = \begin{pmatrix} v_1^1 & v_1^2 \\ v_2^1 & v_2^2 \end{pmatrix} = \begin{pmatrix} 1 & 1 \\ M_1 & M_2 \end{pmatrix},$$

where the components $M_{1,2}$ can be found straightforwardly as

$$M_{1,2} = \frac{q_{22}\gamma_{11} - q_{12}\gamma_{12} - (q_{11}q_{22} - q_{12}^2)\bar{z}_{1,2} + (q_{22} + q_{12})b/\rho s}{q_{12}\gamma_{22} - q_{22}\gamma_{12} + (q_{22} + q_{12})b/\rho s},$$

so that finally

$$\Phi_1 = \Phi_1^* + \Phi_2^*,$$
$$\Phi_2 = M_1\Phi_1^* + M_2\Phi_2^*. \tag{4.9}$$

Shear waves (S-waves)

The last two equations in (4.3) can be rewritten [41] using Biot's non-dimensional parameters (4.5):

$$\overrightarrow{\Psi}_2 = -\frac{\rho_{12} - b/s}{\rho_{22} + b/s}\overrightarrow{\Psi}_1 = -\frac{\gamma_{12} - b/\rho s}{\gamma_{22} + b/\rho s}\overrightarrow{\Psi}_1 = -M_3\overrightarrow{\Psi}_1, \tag{4.10}$$

$$\overrightarrow{\nabla}^2\overrightarrow{\Psi}_1 = \frac{1}{\mu}\left[\rho_{11} - \rho_{12}M_3 + (1 + M_3)\,b/s\right]s^2\overrightarrow{\Psi}_1 \tag{4.11}$$

where $M_3 = \frac{\gamma_{12} - b/\rho s}{\gamma_{22} + b/\rho s}$.

So that finally, we arrive at the wave equation:

$$\overrightarrow{\nabla}^2\overrightarrow{\Psi}_1 = s^2\frac{H}{\mu c^2}\left[\gamma_{11} - \gamma_{12}M_3 + (1 + M_3)\,b/s\right]\overrightarrow{\Psi}_1. \tag{4.12}$$

2D problem

For a 2D problem introduction of the four scalar potentials Φ_1, Φ_2 and Ψ_1, Ψ_2 (Ψ_1 and Ψ_2 are linearly dependent) is sufficient and expressions for the horizontal u_x, U_x and vertical u_z, U_z components of the solid and fluid phase displacements are given by

$$
\begin{aligned}
u_x &= \frac{\partial\Phi_1}{\partial x} + \frac{\partial\Psi_1}{\partial z}, & u_z &= \frac{\partial\Phi_1}{\partial z} - \frac{\partial\Psi_1}{\partial x}, \\
U_x &= \frac{\partial\Phi_2}{\partial x} + \frac{\partial\Psi_2}{\partial z}, & U_z &= \frac{\partial\Phi_2}{\partial z} - \frac{\partial\Psi_2}{\partial x}.
\end{aligned} \tag{4.13}
$$

36

Using potentials in the eigenvector reference system $\mathbf{\Phi}^*$ and $\mathbf{\Psi}^*$ the above expressions become

$$u_x = \frac{\partial \Phi_1^*}{\partial x} + \frac{\partial \Phi_2^*}{\partial x} + \frac{\partial \Psi_1}{\partial z}, \qquad u_z = \frac{\partial \Phi_1^*}{\partial z} + \frac{\partial \Phi_2^*}{\partial z} - \frac{\partial \Psi_1}{\partial x},$$

$$U_x = M_1 \frac{\partial \Phi_1^*}{\partial x} + M_2 \frac{\partial \Phi_2^*}{\partial x} - M_3 \frac{\partial \Psi_2}{\partial z}, \qquad U_z = M_1 \frac{\partial \Phi_1^*}{\partial z} + M_2 \frac{\partial \Phi_2^*}{\partial z} + M_3 \frac{\partial \Psi_1}{\partial x}. \quad (4.14)$$

The components of the strain tensor are

$$\varepsilon_{xx} = \frac{\partial u_x}{\partial x}, \quad \varepsilon_{zz} = \frac{\partial u_z}{\partial z}, \quad \varepsilon_{xz} = \frac{\partial u_x}{\partial z} + \frac{\partial u_z}{\partial x}, \quad \operatorname{tr}\varepsilon = \varepsilon_{xx} + \varepsilon_{zz} = \frac{\partial u_x}{\partial x} + \frac{\partial u_z}{\partial z}.$$

An expression for the stress (2.13) can be written down in terms of the components of a strain tensor ε_{ij}, and $\nabla \cdot \mathbf{u}$, $\nabla \cdot \mathbf{U}$ [9]:

$$\sigma_{ij} = \lambda_f \operatorname{tr}\varepsilon \delta_{ij} + 2\mu\varepsilon_{ij} - M\beta\xi\delta_{ij} = \lambda_f \operatorname{tr}\varepsilon\delta_{ij} + 2\mu\varepsilon_{ij} + M\beta\phi\left[\nabla \cdot (\mathbf{U} - \mathbf{u})\right]\delta_{ij}, \quad (4.15)$$

which can be alternatively written in the form:

$$\begin{aligned}
\sigma_{ij} &= (\lambda_f - M\beta\phi)(\nabla \cdot \mathbf{u})\delta_{ij} + 2\mu\varepsilon_{ij} + M\beta\phi(\nabla \cdot \mathbf{U})\delta_{ij} \\
&= (\lambda + Y)(\nabla \cdot \mathbf{u})\delta_{ij} + 2\mu\varepsilon_{ij} + (R + Y)(\nabla \cdot \mathbf{U})\delta_{ij}, \quad (4.16)
\end{aligned}$$

where $\lambda = \lambda_f + M\phi(\phi - 2\beta) = \lambda_0 + M(\beta - \phi)^2$, $Y = M\phi(\beta - \phi)$, $R = M\phi^2$.

Remark: if we assumed incompressibility of the pore fluid ($M \gg 1$, $\beta = 1$) we would arrive at the relation for the macroscopic stress tensor for incompressible pore fluid, in this case second equation (2.13) gives

$$\nabla \cdot \mathbf{u} = -\nabla \cdot \mathbf{w},$$

or alternatively

$$(1 - \phi)\nabla \cdot \mathbf{u} = -\phi\nabla \cdot \mathbf{U},$$

so that it is easy to see that

$$Y\nabla \cdot \mathbf{u} + R\nabla \cdot \mathbf{U} = \mathbf{0}$$

and the relation for the stress tensor becomes

$$\sigma_{ij} = \lambda(\nabla \cdot \mathbf{u})\delta_{ij} + 2\mu\varepsilon_{ij} + Y(\nabla \cdot \mathbf{U})\delta_{ij}.$$

In the present work the general relation for Hooke's law (4.15) will be used, so that components of the stress tensor can be related to the scalar potentials in the following way:

$$
\begin{aligned}
\sigma_{xx} &= (\lambda + Y)\nabla^2\Phi_1 + (R + Y)\nabla^2\Phi_2 + 2\mu\left(\frac{\partial^2\Phi_1}{\partial x^2} + \frac{\partial^2\Psi_1}{\partial x \partial z}\right), \\
\sigma_{zz} &= (\lambda + Y)\nabla^2\Phi_1 + (R + Y)\nabla^2\Phi_2 + 2\mu\left(\frac{\partial^2\Phi_1}{\partial z^2} - \frac{\partial^2\Psi_1}{\partial x \partial z}\right), \\
\sigma_{xz} &= \mu\left(2\frac{\partial^2\Phi_1}{\partial x \partial z} + \frac{\partial^2\Psi_1}{\partial z^2} - \frac{\partial^2\Psi_1}{\partial x^2}\right).
\end{aligned}
\tag{4.17}
$$

Pore pressure can be expressed in a similar way:

$$
\begin{aligned}
p &= M(-\beta\operatorname{tr}\varepsilon + \xi) = -M\left[(\beta - \phi)\nabla \cdot \mathbf{u} + \phi\nabla \cdot \mathbf{U}\right] = \\
&= -\frac{1}{\phi}\left[Y\nabla \cdot \mathbf{u} + R\nabla \cdot \mathbf{U}\right] = -\frac{1}{\phi}\left[Y\nabla^2\Phi_1 + R\nabla^2\Phi_2\right].
\end{aligned}
\tag{4.18}
$$

As a result of the above transformations, the 2D problem (similar techniques may be used for the axially symmetric case and fully 3D case) for the governing equations (2.23), (2.24) was reduced to the wave equations (4.8), (4.12) for three unknown scalar potentials: two dilatational - Φ_1, Φ_2 (or Φ_1^*, Φ_2^* in the eigenvector reference system) and one shear Ψ_1.

4.2 General solution of the 2D problem

Consider, at first, the general problem which includes dissipation effects. A poroelastic half-space occupying the region $z < 0$ is subjected to an impulsive external traction $P(x)$ at the surface. The boundary conditions for the governing equations (4.1)

and stress-strain relation (4.15) can be represented in the following way ($z = 0$):

$$\begin{aligned}
\sigma_{zz}(x, 0, t) &= -P(x)\delta(t), \\
\sigma_{xz}(x, 0, t) &= 0, \\
p(x, 0, t) &= Q(x)\delta(t),
\end{aligned} \tag{4.19}$$

so that $P(x)$ represents the external load and varying the values for $Q(x)$ one can obtain either solution for the permeable piston problem [33] (setting $Q = 0$), or for the liquid piston problem (setting $Q(x) = P(x)$) [41]. For point sources (axial symmetry case), as was done, for example, in [23], one should consider $P(x) = P_0\delta(x)$ and $Q(x) = Q_0\delta(x)$.

As was shown above, the 2D problem reduces to the solution of the wave equations in Laplace space:

$$\beta_1^2 \nabla^2 \Phi_1^* = s^2 \Phi_1^*, \quad \beta_2^2 \nabla^2 \Phi_2^* = s^2 \Phi_2^*, \quad \beta_3^2 \nabla^2 \Psi_1 = s^2 \Psi_1, \tag{4.20}$$

where β_1, β_2, β_3 represent P1, P2 and shear waves velocities, respectively, so that

$$\begin{aligned}
\beta_1 &= V_{p1}(s) = \frac{c}{\sqrt{\bar{z}_1}}, \quad \beta_2 = V_{p2}(s) = \frac{c}{\sqrt{\bar{z}_1}}, \\
\beta_3 &= V_S(s) = \sqrt{\frac{\mu}{\rho_{11} - \rho_{12}M_3 + (1 + M_3)\,b/s}} = \sqrt{\frac{\mu}{\rho}}\sqrt{\frac{1}{\gamma_{11} - \gamma_{12}M_3 + (1 + M_3)\,b/\rho s}}.
\end{aligned}$$

Equations (4.20), written down in Fourier space with a Fourier transform defined as

$$f(k) = \frac{1}{\sqrt{2\pi}} \int_{-\infty}^{+\infty} f(x)e^{-ikx}\,dk, \qquad f(x) = \frac{1}{\sqrt{2\pi}} \int_{-\infty}^{+\infty} f(k)e^{ikx}\,dx$$

become (here and henceforth, transformed solutions will be indicated by the arguments)

$$\frac{\partial^2 \Phi_{1,2}^*(k, z, s)}{\partial z^2} = \left(k^2 + \frac{s^2}{\beta_{1,2}^2}\right)\Phi_{1,2}^*(k, z, s), \quad \frac{\partial^2 \Psi_1(k, z, s)}{\partial z^2} = \left(k^2 + \frac{s^2}{\beta_3^2}\right)\Psi_1,$$
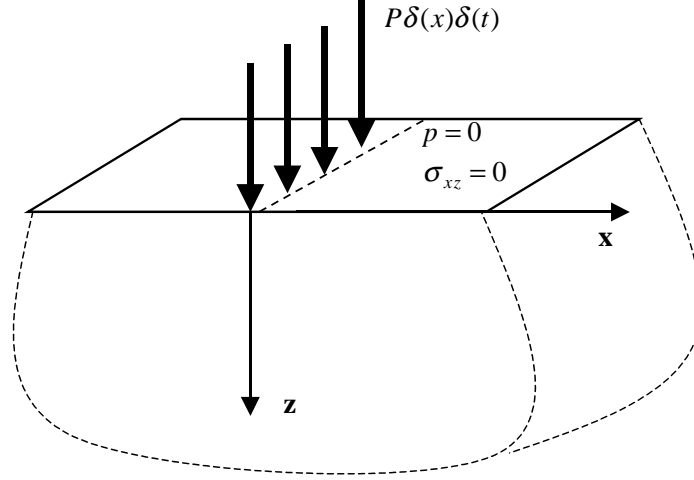
39

Figure 4.1: Line surface traction. Scheme to the statement of the problem.

so that taking into account far field conditions at infinity

$$[\operatorname{div}\mathbf{u}]_\infty = 0, \quad [\operatorname{curl}\mathbf{u}]_\infty = 0,$$

solutions of the above wave equations can be expressed in the form:

$$\Phi^*_{1,2}(k,z,s) = A_{1,2}(k,s)\exp\left[-z\cdot\xi_{1,2}(k,s)\right], \quad \Psi_1(k,z,s) = B(k,s)\exp\left[-z\cdot\xi_3(k,s)\right], \tag{4.21}$$

where $\xi_i(k,s) = \sqrt{k^2 + \frac{s^2}{\beta_i^2}}$ $(i = 1,2,3)$, $A_{1,2}(k,s)$ and $B(k,s)$ are unknown coefficients to be determined from the boundary conditions.

In the Laplace-Fourier space the expressions for the stress tensor and the pressure in terms of the potentials (4.20) can be written down as

$$
\begin{aligned}
\sigma_{zz}(k,z,s) &= (\lambda + Y)\left[-k^2\Phi^*_1 - k^2\Phi^*_2 + \xi_1^2(k,s)\Phi^*_1 + \xi_2^2(k,s)\Phi^*_2\right] + \\
&\quad + (R+Y)\left[-k^2 M_1\Phi^*_1 - k^2 M_2\Phi^*_2 + M_1\xi_1^2(k,s)\Phi^*_1 + M_2\xi_2^2(k,s)\Phi^*_2\right] + \\
&\quad + 2\mu\left[\xi_1^2(k,s)\Phi^*_1 + \xi_2^2(k,s)\Phi^*_2 + ik\xi_3(k,s)\Psi_1\right], \tag{4.22}\\
\sigma_{xz}(k,z,s) &= \mu\left(-2ik\xi_1(k,s)\Phi^*_1 - 2ik\xi_2(k,s)\Phi^*_2 + \xi_3^2(k,s)\Psi_1 + k^2\Psi_1\right), \\
p(k,z,s) &= -\frac{1}{\phi}Y\left[-k^2\Phi^*_1 - k^2\Phi^*_2 + \xi_1^2(k,s)\Phi^*_1 + \xi_2^2(k,s)\Phi^*_2\right] - \\
&\quad - \frac{1}{\phi}R\left[-k^2 M_1\Phi^*_1 - k^2 M_2\Phi^*_2 + M_1\xi_1^2(k,s)\Phi^*_1 + M_2\xi_2^2(k,s)\Phi^*_2\right].
\end{aligned}
$$

So that applying boundary conditions (4.19) one can get the following system for the three unknown coefficients $A_{1,2}(k,s)$ and $B(k,s)$:

$$A_1(k,s)\left[(m_1+n_1)\,s^2+k^2\right]+A_2(k,s)\left[(m_2+n_2)\,s^2+k^2\right]+B(k,s)ik\xi_3(k,s)=-\frac{P(k)}{2\mu},$$

$$A_1(k,s)2ik\xi_1(k,s)+A_2(k,s)2ik\xi_2(k,s)-B(k,s)\left(2k^2+\frac{s^2}{\beta_3^2}\right)=0,$$

$$A_1(k,s)n_1s^2+A_2(k,s)n_2s^2=-\frac{\phi Q(k)}{2\mu}, \tag{4.23}$$

where

$$m_{1,2}=\frac{\lambda+2\mu+YM_{1,2}}{2\mu\beta_{1,2}^2},\quad n_{1,2}=\frac{Y+RM_{1,2}}{2\mu\beta_{1,2}^2}.$$

Setting $Q=0$ for simplicity one can get the following solution of the system (4.23):

$$A_1(k,s) = \frac{P(k)}{2\mu}\frac{n_2\left(2k^2+\frac{s^2}{\beta_3^2}\right)}{F(k,s)},\quad A_2(k,s)=-\frac{P(k)}{2\mu}\frac{n_1\left(2k^2+\frac{s^2}{\beta_3^2}\right)}{F(k,s)},$$

$$B(k,s) = -2ik\frac{P(k)}{2\mu}\frac{n_1\xi_2(k,s)-n_2\xi_1(k,s)}{F(k,s)}, \tag{4.24}$$

where $F(k,s)$ is the dispersion relation of the surface (Rayleigh) waves:

$$F(k,s)=\left(2k^2+\frac{s^2}{\beta_3^2}\right)\left[n_1(m_2s^2+k^2)-n_2(m_1s^2+k^2)\right]-2k^2\xi_3(n_1\xi_2-n_2\xi_1). \tag{4.25}$$

This equation, written down in a similar way can be found in [41], however, results obtained by Paul [33] for the zero dissipation case ($b=0$) were presented in the alternate form:

$$F^*(k,s)=\left(2k^2+\frac{s^2}{\beta_3^2}\right)^2-4k^2\xi_3\left(K_1\xi_2-K_2\xi_1\right). \tag{4.26}$$

41

There is no contradiction as the connection between the two representations can be elucidated by the following normalization of the coefficients n_2, n_2:

$$K_{1,2} = \frac{n_{1,2}}{(n_1 - n_2)}.$$

It can be shown (either numerically or analytically) that for the case of no dissipation ($b = 0$) the following identity holds:

$$2\frac{n_1 m_2 - n_2 m_1}{(n_1 - n_2)} = \frac{1}{\beta_3^2}, \tag{4.27}$$

so that both formulations are equivalent. Moreover, the above expression (4.27) gives the connection between the phase velocities of the P1, P2 and S waves and poroelastic parameters of the media for the zero dissipation case.

It has been shown, that for the no dissipation case equation (4.25) has only one real positive root, which corresponds to the surface wave mode [14], [43], [41].

Solid and fluid phase displacements **u** and **U**, following (4.14) and (4.21), can be expressed as follows:

$$
\begin{aligned}
u_x(k,z,s) &= ikA_1(k,s)e^{-z\cdot\xi_1(k,s)} + ikA_2(k,s)e^{-z\cdot\xi_2(k,s)} - \xi_3(k,s)B(k,s)e^{-z\cdot\xi_3(k,s)}, \\
u_z(k,z,s) &= -\xi_1(k,s)A_1(k,s)e^{-z\cdot\xi_1(k,s)} - \xi_2(k,s)A_2(k,s)e^{-z\cdot\xi_2(k,s)} - \\
&\quad -ikB(k,s)e^{-z\cdot\xi_3(k,s)}, \\
U_x(k,z,s) &= ikM_1A_1(k,s)e^{-z\cdot\xi_1(k,s)} + ikM_2A_2(k,s)e^{-z\cdot\xi_2(k,s)} + \\
&\quad +M_3\xi_3(k,s)B(k,s)e^{-z\cdot\xi_3(k,s)}, \\
U_z(k,z,s) &= -M_1\xi_1(k,s)A_1(k,s)e^{-z\cdot\xi_1(k,s)} - M_2\xi_2(k,s)A_2(k,s)e^{-z\cdot\xi_2(k,s)} + \\
&\quad +ikM_3B(k,s)e^{-z\cdot\xi_3(k,s)}.
\end{aligned}
\tag{4.28}
$$

So that using the values of the coefficients A_1, A_2 and B, (4.24), the solution in the Laplace space can be represented in the form:

$$u_x(x,z,s) = \frac{1}{2\mu\sqrt{2\pi}} \int\limits_{-\infty}^{+\infty} \frac{P(k)}{F(k,s)} \left\{ ik \left(2k^2 + \frac{s^2}{\beta_3^2} \right) \left[n_2 e^{-z\cdot\xi_1(k,s)} - n_1 e^{-z\cdot\xi_2(k,s)} \right] + \right.$$

$$\left. +2ik\xi_3(k,s) \left[n_1\xi_2(k,s) - n_2\xi_1(k,s) \right] e^{-z\cdot\xi_3(k,s)} \right\} e^{ikx} dk,$$

$$u_z(x,z,s) = -\frac{1}{2\mu\sqrt{2\pi}} \int\limits_{-\infty}^{+\infty} \frac{P(k)}{F(k,s)} \left\{ \left(2k^2 + \frac{s^2}{\beta_3^2} \right) \left[n_2\xi_1(k,s) e^{-z\cdot\xi_1(k,s)} - \right. \right. \tag{4.29}$$

$$\left. \left. - n_1\xi_2(k,s) e^{-z\cdot\xi_2(k,s)} \right] + 2k^2 \left[n_1\xi_2(k,s) - n_2\xi_1(k,s) \right] e^{-z\cdot\xi_3(k,s)} \right\} e^{ikx} dk,$$

$$U_x(x,z,s) = \frac{1}{2\mu\sqrt{2\pi}} \int\limits_{-\infty}^{+\infty} \frac{P(k)}{F(k,s)} \left\{ ik \left(2k^2 + \frac{s^2}{\beta_3^2} \right) \left[n_2 M_1 e^{-z\cdot\xi_1(k,s)} - n_1 M_2 e^{-z\cdot\xi_2(k,s)} \right] - \right.$$

$$\left. -2ik M_3 \xi_3(k,s) \left[n_1\xi_2(k,s) - n_2\xi_1(k,s) \right] e^{-z\cdot\xi_3(k,s)} \right\} e^{ikx} dk,$$

$$U_z(x,z,s) = -\frac{1}{2\mu\sqrt{2\pi}} \int\limits_{-\infty}^{+\infty} \frac{P(k)}{F(k,s)} \left\{ \left(2k^2 + \frac{s^2}{\beta_3^2} \right) \left[n_2 M_1 \xi_1(k,s) e^{-z\cdot\xi_1(k,s)} - \right. \right.$$

$$\left. \left. - n_1 M_2 \xi_2(k,s) e^{-z\cdot\xi_2(k,s)} \right] -2k^2 M_3 \left[n_1\xi_2(k,s) - n_2\xi_1(k,s) \right] e^{-z\cdot\xi_3(k,s)} \right\} e^{ikx} dk.$$

Similarly, one can get the expressions for the components of the stress tensor as well as for the pore pressure. The above general solution is valid for either no dissipation case or for the case when dissipation is present. In the latter case the coefficients n_1, n_2, m_1, m_2, M_1, M_2, M_3 become complex numbers and will depend on frequency. It will be shown in the following that a semianalytic solution is possible for the steady - state source, and a closed form solution can be derived for the Green's function in the case of no dissipation.

For the overall displacements $\mathbf{u}$ (4.29) it is always possible to show the connection between the solutions obtained for the porous medium and known solutions for the perfectly elastic case. This was analyzed, for example, in [33] and [41] (detailed discussion of the limiting cases of Biot's equations is presented in [9]).

Limiting Case. Benchmark solution.

Setting $\beta = \phi = 0$, $b = 0$, so that $Y = R = 0$ and $\rho_{11} = \rho_{22} = 0$, governing equations for the porous medium (4.1) degenerate into the equations of a perfect solid [9]. In this case we have $\beta_1 = \beta_2$, $m_1 = m_2 = \frac{1}{2}\frac{\lambda+2\mu}{\mu\beta_1^2} = \frac{1}{2}\frac{\beta_1^2}{\beta_3^2\beta_1^2} = \frac{1}{2\beta_3^2}$, so that

equation (4.25) becomes

$$F(k, s) = \frac{1}{2} (n_1 - n_2) \left[\left(2k^2 + \frac{s^2}{\beta_3^2} \right)^2 - 4k^2 \xi_1 \xi_3 \right],$$ (4.30)

where the expression in the square brackets can be recognized as the well-known Rayleigh wave equation [1]. Finally, expressions for the overall displacements **u** (4.29) evaluated at the surface $z = 0$ become

$$u_x(x, 0, s) = -\frac{1}{\mu \sqrt{2\pi}} \int\limits_{-\infty}^{+\infty} \frac{ikP(k)}{R(k, s)} \left[\left(2k^2 + \frac{s^2}{\beta_3^2} \right) - 2\xi_1(k, s)\xi_3(k, s) \right] e^{ikx} dk,$$

$$u_z(x, 0, s) = \frac{1}{\mu \sqrt{2\pi}} \int\limits_{-\infty}^{+\infty} \frac{P(k)}{R(k, s)} \frac{s^2}{\beta_3^2} \xi_1(k, s) e^{ikx} dk.$$ (4.31)

These represent the Laplace transformed solution of Lamb's problem for the perfectly elastic solid [26], [41].

4.2.1 Surface waves

The dispersion relation governing the propagation of the surface waves in the general frequency dependent form (4.25) was first analyzed by Deresiewicz [13]. For non-dissipative media it appears in the form (4.26) in the following works, [43], [33], [14]. In the works dedicated to the solution of boundary value problems, for example [41], [23], it arises in its general frequency dependent form.

A nondimensional form of the obtained above equation (4.25), can be written down in terms of the non dimensional horizontal slowness p [1], so that k and s in (4.25) are replaced by $k = \frac{\omega p}{\beta_3}$, $s = i\omega$. In this case we have

$$\tilde{F}(p, \tilde{\omega}) = \left(2p^2 - 1 \right) \left[\tilde{n}_1 \varsigma_1^2 \left(p^2 - \tilde{m}_2 \varsigma_2^2 \right) - \tilde{n}_2 \varsigma_2^2 (p^2 - \tilde{m}_1 \varsigma_1^2) \right] -$$
$$- 2p^2 \sqrt{p^2 - 1} \left(\tilde{n}_1 \varsigma_1^2 \sqrt{p^2 - \varsigma_2^2} - \tilde{n}_2 \varsigma_2^2 \sqrt{p^2 - \varsigma_1^2} \right),$$ (4.32)
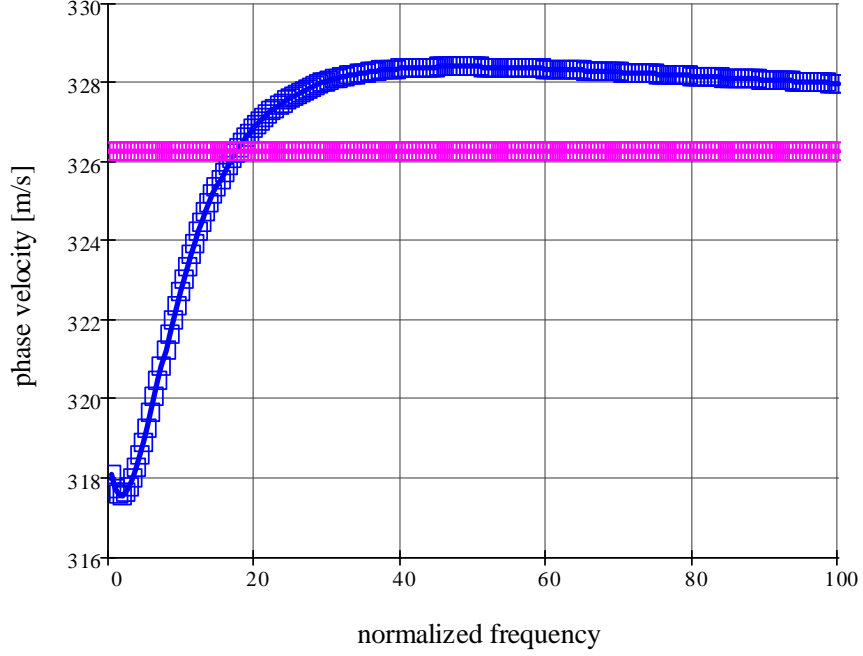
where

Figure 4.2: Fatt's model. Rayleigh wave phase velocity versus normalized frequency $\frac{\rho}{b}\omega$. The straight line represents the case of no dissipation case $(\omega \to \infty)$

$$\varsigma_1 = \frac{\beta_3}{\beta_2}, \quad \varsigma_2 = \frac{\beta_3}{\beta_1}, \quad \tilde{n}_{1,2} = \frac{Y + RM_{1,2}}{2\mu}, \quad \tilde{m}_{1,2} = \frac{\lambda + 2\mu + YM_{1,2}}{2\mu},$$

$$\tilde{\omega} = \frac{\rho\omega}{b}, \quad M_{1,2} = \frac{q_{22}\gamma_{11} - q_{12}\gamma_{12} - (q_{11}q_{22} - q_{12}^2)\bar{z}_{1,2} - \frac{i}{\tilde{\omega}}(q_{22} + q_{12})}{q_{12}\gamma_{22} - q_{22}\gamma_{12} - \frac{i}{\tilde{\omega}}(q_{22} + q_{12})\tilde{\omega}}. \quad (4.33)$$

The characteristic frequency for a given material is given by

$$\omega_c = \frac{b}{\rho}.$$

For the Fatt's model it is approximately $63.2kHz$ while for the water saturated Berea sandstone it is approximately $48.0kHz$.

Generally speaking, the coefficients $\tilde{n}_1$, $\tilde{n}_2$, $\tilde{m}_1$, $\tilde{m}_2$ are functions of the non dimensional frequency $\tilde{\omega}$, however, for the no dissipation case they become constants, so that using relation (4.27), the nondimensional form of equation (4.26) can be represented in the following way:
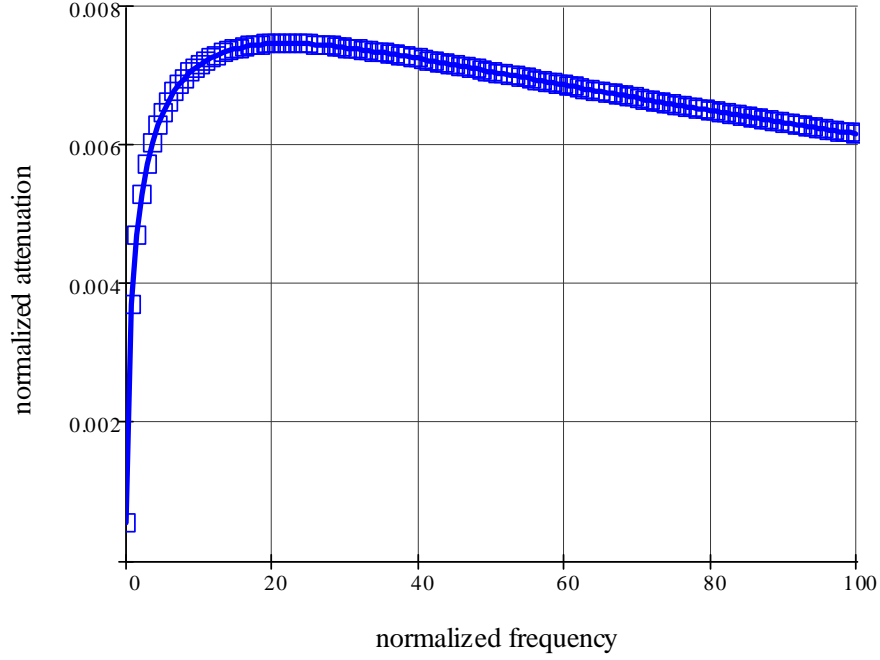
Figure 4.3: Fatt's model. Rayleigh wave attenuation coefficient versus normalized frequency $\frac{\rho}{b}\omega$

$$\tilde{F}^*(x) = (2x-1)^2 - 4x\sqrt{x-1}\left(K_1\sqrt{x-\varsigma_2^2} - K_2\sqrt{x-\varsigma_1^2}\right), \qquad (4.34)$$

where $K_1 = \frac{\tilde{n}_1\varsigma_1^2}{\tilde{n}_1\varsigma_1^2 - \tilde{n}_2\varsigma_2^2}$, $K_2 = \frac{\tilde{n}_2\varsigma_2^2}{\tilde{n}_1\varsigma_1^2 - \tilde{n}_2\varsigma_2^2}$, $x = p^2$.

Non-dissipative case

First of all, consider the case of no dissipation ($\tilde{\omega} = 0$). In this case the surface wave is non dispersive and propagates with a constant velocity. For the poroelastic parameters obtained for kerosene saturated sandstone [16] one can calculate the physical values for the P1, P2, S and surface wave phase velocities. In this case coefficients $\tilde{n}_1$, $\tilde{n}_2$, $\tilde{m}_1$, $\tilde{m}_2$ can be found to equal $\tilde{n}_1 = 0.187$, $\tilde{n}_2 = -0.476$, $\tilde{m}_1 = 1.925$, $\tilde{m}_2 = 0.417$ so that

$$\beta_1 = 706.346\frac{m}{s}, \beta_2 = 326.771\frac{m}{s}, \beta_3 = 359.788\frac{m}{s}.$$

The dispersion equation (4.32) has only one real positive root which can be calculated numerically: $p_R = 1.10276$ ($p_R = 1.103$ [41]), so that the surface wave phase velocity is $\beta_4 = \frac{\beta_3}{p_R} = 326.262\frac{m}{s}$ ($\beta_4 = 326.19\frac{m}{s}$ [41]). It was shown [43] (for different Poisson's coefficient values), [41] that for the Fatt's model the phase velocity of the surface wave is larger compared to the Rayleigh wave in a perfectly elastic solid with the corresponding elastic parameters.

Results for the Berea sandstone set of parameters are different. In this case the dispersion equation (4.34) has no roots. A simple procedure was used to demonstrate this: one can obtain a polynomial corresponding to the dispersion relation (4.34) by multiplying this equation by its conjugate twice, so that the square roots can be eliminated. The coefficients of this polynomial are given in Appendix B. It is easy to see that the leading order coefficient is identically zero (as by definition we have: $K_1 - K_2 = 1$), so that application of, for example, LaGuerre's method will give all 7 roots, afterwards spurious roots have to be rejected by substitution into the initial equation (4.34).

Further, with application of the Cagniard de Hoop technique, it will be shown that the absence of the root of the secular equation does not necessarily imply that there is no Rayleigh wave. In this particular case it will still appear as a consequence of very small values taken by the dispersion function $\tilde{F}^*(p)$ in the vicinity of the desired contour in the complex p plane.

Dissipative case

It is also important to obtain characteristics of the surface wave in the case when the connection between phases is pronounced. Non zero dissipation ($b > 0$, $\tilde{\omega} > 0$) results in a frequency dependence of the coefficients $\tilde{n}_1$, $\tilde{n}_2$, $\tilde{m}_1$, $\tilde{m}_2$ so that the surface wave become dispersive. Numerical analysis of equation (4.32) with Fatt's parameters gives, in general, one main complex root p_R (see Figures 4.2, 4.3) so that $\mathrm{Re}\left(\frac{\beta_3}{p_R}\right)$ will represent the dimensional phase velocity of the surface wave, and $\left|\mathrm{Im}\left(\frac{1}{p_R}\right)\right|$ corresponds to the normalized attenuation.

Thus, when dissipation effects are taken into account, the surface wave is always attenuated and, therefore will be less pronounced. The velocity of propagation of this wave can be determined for all $0 < \omega < \infty$. The phase velocity of the Rayleigh wave is always smaller than the phase velocity of the shear S-wave (see
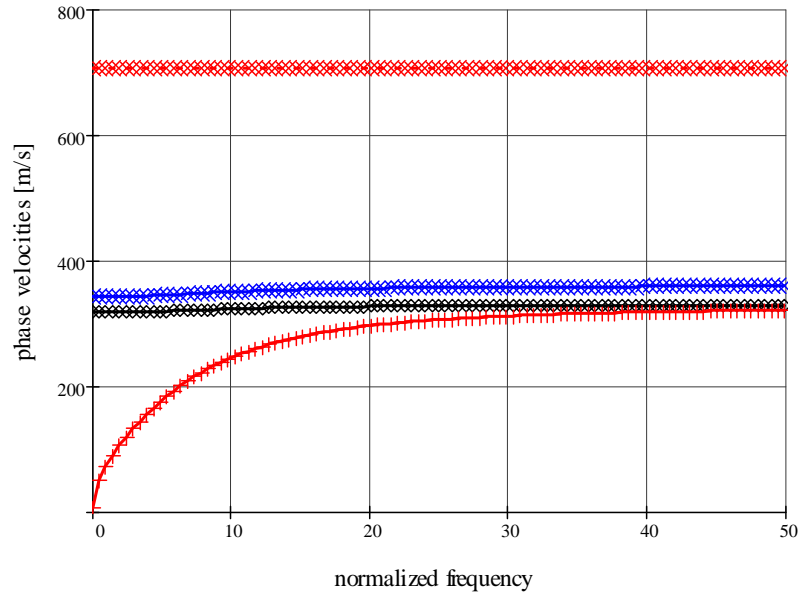
Figure 4.4: Fatt's model. Phase velocities (P1 red x, S blue x, Rayleigh black x, P2 red +) versus non-dimensional frequency $\frac{\rho}{b}\omega$

Figures 4.4, 4.5). As a function of ω, it possesses an inflection point and is slightly non monotonic in the range of small frequencies. The velocity possesses a weak minimum (see Figure 4.2) at low frequencies and a broad maximum near $\omega \approx 40$.

As mentioned above, when viscous effects are included, the Rayleigh wave will always be attenuated, this means that it is an example of a leaky wave [1]. The attenuation of this wave grows from zero for $\omega \to 0$ and reaches a maximum at approximately 20 characteristic frequencies and monotonically decays further so that $\omega \to \infty$ will give zero attenuation (this limit corresponds to the non-dissipative case).

Thus, the damped dispersive surface waves may propagate faster (high frequency range) or slower (low frequency range) compared to non dispersive ones (see Figure 4.4). The phase velocity of the surface wave in the Fatt's model varies in the following range: $\approx 317.6\frac{m}{s} - 328.5\frac{m}{s}$, while the non dissipative propagation speed was determined above as $\approx 326.262\frac{m}{s}$.

Similar results were obtained for the Berea sandstone poroelastic parameters (see Appendix E.2). Figures 4.4, 4.5 represent dimensional phase velocities versus normalized frequency for both Fatt's model and the Berea sandstone. However,
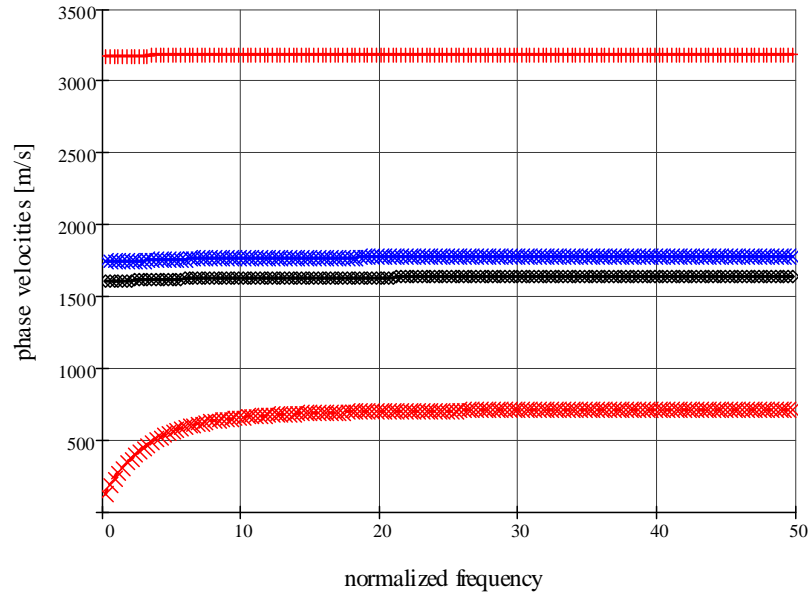
Figure 4.5: Water saturated Berea sandstone. Phase velocities (P1, S, Rayleigh, P2) versus non-dimensional frequency $\frac{\rho}{b}\omega$

results obtained for the two sets of physical parameters should be extrapolated to other cases with great care. For example, in the case of the Berea sandstone equation (4.34) has no roots.

The main conclusion, justified with two sets of parameters is that while phase velocity and attenuation are observed to rise with increasing frequencies for P1, P2 and S wave motion (see [6], [9]) Rayleigh wave propagation speed and attenuation are not monotonic.

4.3 Steady-state harmonic line traction

Boundary value problems for steady state response of the poroelastic half-space in the framework of Biot's theory were considered in [23], [14], [36], [45]. In [14] results were obtained for a simplified model with viscous dissipation neglected. In [14] 2D problem was considered for a non-dissipative medium, however, the main focus was on the stress distribution at the surface. In [45] an analytic solution was presented for both displacements and stresses.

Dissipation effects were taken into account by Halpern and Christiano [23] for the axially symmetric problem. Results for the point traction were summarized in the form of the approximate (far field) Green's function matrix which was evaluated numerically at the surface as a function of the source frequency. It was reported that the exact Green's functions for the point load is represented by divergent integrals and as a remedy it was suggested to approximate Green's functions with some modified (exponentially decaying) distributions of the surface traction. Valliapan *et al.* [45] obtained analytic solutions without application of Helmholtz potentials. In this work numerical results were presented for solid phase and filtration amplitudes as well as for the stresses, calculated not only at the surface but also in the interior of the domain. Unlike [45], in the present study the emphasis is made on the analysis of the response at different source frequencies.

2D line traction is considered for a porous half-space with a free boundary pressure. Exact (valid for any source - receiver distance) Green's functions are presented for a wide range of source frequencies. The results of numerical calculations of the obtained analytical solution are presented for the vertical solid and fluid phase displacements for a line source distributed over the interval $-l < x < l$.

In the present work emphasis is made on the analysis of the displacement field for different source frequencies. Obviously, in the case of well pronounced coupling between phases (due to the fluid viscosity, or low porosity and permeability) one can expect both phases moving together, so that filtration will be relatively small, however, in the case of relatively high source frequencies (approximately 100 kHz) this coupling will be far less pronounced.

Solution (4.29) can be used to obtain a half-space response to a steady-state harmonic line source. In this particular case we assume harmonic time dependence for the displacements as well as for the components of the total stress tensor and pore pressure. So that the boundary conditions (4.19) become

$$\sigma_{zz}(x,0,t) = -P(x)e^{i\omega t}, \ \ \sigma_{xz}(x,0,t) = 0, \ \ p(x,0,t) = Q(x)e^{i\omega t} \tag{4.35}$$

and the solution (4.29), obtained for $Q(x) = 0$ (open interface) can be used.

Solution of the harmonic surface line traction problem can be obtained based on the general solution (4.29). In this particular case, one gets the following expressions for the solid and fluid phase displacements at the surface ($z = 0$) in the physical domain:

$$u_z(x,0,t) = \frac{1}{\mu\sqrt{2\pi}}\text{Re}\left\{e^{i\omega t}\int\limits_{-\infty}^{+\infty}\frac{P(k)\omega^2}{\beta_3^2}\frac{n_2\xi_1(k,\omega)-n_1\xi_2(k,\omega)}{F(k,\omega)}e^{ikx}dk\right\},$$

$$U_z(x,0,t) = -\frac{1}{\mu\sqrt{2\pi}}\text{Re}\left\{e^{i\omega t}\int\limits_{-\infty}^{+\infty}\frac{P(k)}{F(k,\omega)}\left[n_2\xi_1(k,\omega)\left(2k^2(M_1+M_3)-M_1\frac{\omega^2}{\beta_3^2}\right)-\right.\right.$$
$$\left.\left.-n_1\xi_2(k,\omega)\left(2k^2(M_2+M_3)-M_2\frac{\omega^2}{\beta_3^2}\right)\right]e^{ikx}dk\right\}, \tag{4.36}$$

where $\xi_i(k,\omega) = \sqrt{k^2-\frac{\omega^2}{\beta_i^2}}$ ($i=1,2,3$) and $F(k,\omega)$ is obtained from the Rayleigh wave secular equation $F(k,s)$ by the substitution $s=i\omega$.

At first, consider the solution in the case of line traction (see Figure 4.1). In this case $P(x)=P\delta(x)$, where P denotes a constant, so that in Fourier space we have $P(k)=\frac{P}{\sqrt{2\pi}}$ (P has dimensions of force per unit length). The change of variable $k=\frac{\omega p}{\beta_3}$, as was done in a Section 4.2.1, leads to expressions for the non-dimensional vertical displacements $\tilde{u}_z = \frac{4\pi\mu}{P}u_z$ and $\tilde{U}_z = \frac{4\pi\mu}{P}U_z$ in the form:

$$u_z(x,t,\omega) = \text{Re}\int\limits_{-\infty}^{+\infty}\frac{n_2\varsigma_2^2\xi_1(p)-n_1\varsigma_1^2\xi_2(p)}{F(p,\omega)}e^{i(px+t)}dp,$$

$$U_z(x,t,\omega) = -\text{Re}\int\limits_{-\infty}^{+\infty}\frac{1}{F(p,\omega)}\left\{n_2\varsigma_2^2\xi_1(p)\left[2p^2(M_1+M_3)-M_1\right]-\right.$$
$$\left.-n_1\varsigma_1^2\xi_2(p)\left[2p^2(M_2+M_3)-M_2\right]\right\}e^{i(px+t)}dp, \tag{4.37}$$

where $\xi_{1,2}(p) = \sqrt{p^2-\varsigma_{1,2}^2}$, $F(p,\omega)$ is the non-dimensionalized surface wave equation (4.32) and the following non-dimensional quantities are used: $\tilde{x} = \frac{\omega x}{\beta_3}$, $\tilde{t} = \omega t$ (tildes are omitted in (4.37)). The non-dimensional frequency $\tilde{\omega}$ in (4.37) was defined in (4.32) as

$$\tilde{\omega} = \frac{\rho}{b}\omega = \frac{\rho k}{\eta\phi^2}\omega = \frac{\omega}{\omega_c}, \tag{4.38}$$

where $\omega_c = \frac{\eta\phi^2}{\rho k}$ is the characteristic or roll-over frequency, ϕ - porosity, η - saturating fluid viscosity, k - permeability and a - tortuosity.

Green's functions

The solution (4.37) for the line source is represented in the form of slowly decaying, highly-ocsillating integrals. It can be shown that the integrand amplitudes have $\frac{1}{p}$ asymptotics for large p, so that special care has to be taken in the case of numerical evaluation. Halpern and Christiano [23] reported divergent integrals in the case of the corresponding axially symmetric steady state Lamb's problem. As a remedy, a special shape of the loading which approximates Dirac's function was suggested. Solutions for the far field Green's function were presented and analyzed. Some conclusions in [23] are speculative, for example, it was mentioned, that even a uniform traction distributed over a finite circular area will cause divergence of the integrals. Later studies, Valliappan *et al.* [45] and the present study demonstrate the contrary.

First of all, consider the asymptotic expansion of the amplitudes in the expression for the solid and fluid phase displacements (4.37):

$$\frac{n_2 \varsigma_2^2 \xi_1(p) - n_1 \varsigma_1^2 \xi_2(p)}{F(p, \omega)} \approx A_s(\omega)\frac{1}{p} + O\left(\frac{1}{p^3}\right),$$

$$\frac{n_2 \xi_1(p)\left[2p^2(M_1 + M_3) - M_1\right] - n_1 \varsigma_1^2 \xi_2(p)\left[2p^2(M_2 + M_3) - M_2\right]}{F(p, \omega)} \approx A_f(\omega)\frac{1}{p} + O\left(\frac{1}{p^3}\right),$$

$$(4.39)$$

where the leading order coefficients $A_s(\omega)$ and $A_f(\omega)$ can be evaluated exactly, for example,

$$A_s(\omega) = \frac{n_2 \varsigma_2^2 - n_1 \varsigma_1^2}{\varsigma_1^2 \varsigma_2^2 \left(2n_2 m_1 - 2n_1 m_2 + n_1 - n_2\right)}.$$

Thus, we need to investigate the convergence at infinity of integrals of the type

$$\int\limits_a^\infty \frac{\sin(px)}{p}\,dp, \qquad \int\limits_a^\infty \frac{\cos(px)}{p}\,dp,$$

where $a > 0$. The above integrals can be evaluated exactly in terms of the special sine and cosine integral functions $\mathrm{Si}(x)$ and $\mathrm{Ci}(x)$ [21] which are defined as

$$\mathrm{Si}(x) = \int\limits_0^x \frac{\sin(p)}{p}\,dp = \frac{\pi}{2} - \int\limits_x^\infty \frac{\sin(p)}{p}\,dp, \qquad \mathrm{Ci}(x) = -\int\limits_x^\infty \frac{\cos(p)}{p}\,dt,$$

52

so that we can write

$$\int_a^\infty \frac{\sin(px)}{p}\,dp = \frac{\pi}{2} - \text{Si}(ax), \qquad \int_a^\infty \frac{\cos(px)}{p}\,dp = -\text{Ci}(ax).$$

The above expressions are useful in estimation of the highly oscillating "tails" of the integrals (4.37) for sufficiently large a.

It can thus be concluded that Green's functions can be presented in the form of slowly decaying highly oscillating but nevertheless convergent integrals (divergence only occurs at $x = 0$, where the traction is applied). Numerical evaluation of the slowly decaying, highly oscillating integrals requires special care. The results reported by Halpern and Christiano [23] can be argued against also from a physical standpoint - infinitely large displacements can not be caused by an ocsillating point traction of a finite amplitude for a stable material.

Numerical calculations for the exact Green's function are presented in Appendix C. At the point $x = 0$, an integrable singularity can be observed, which disappears in the case of a uniformly distributed traction. The range of the source frequencies used in calculations varies from $\omega = 0.1\omega_c$ to $\omega = 100\omega_c$. Further increase of the source frequency gives out of phase motion similar to that presented in Figure C.4.

Distributed source

We now consider a traction which is distributed over the interval $(-l < x < l)$. In this case one can obtain well-convergent Cauchy type integrals with $\frac{1}{p^2}$ asymptotics at infinity.

For the distributed line traction, instead of $\sigma_{zz}(x, 0, t) = -P(k)e^{i\omega t}$ in (4.35) we have

$$\sigma_{zz}(x, 0, t) = \begin{cases} P, & |x| < l \\ 0, & |x| > l \end{cases}$$

where P is some constant to describe the power of the loading (P has dimension of force per unit area), so that in Fourier space

$$\sigma_{zz}(k, 0, t) = P\sqrt{\frac{2}{\pi}}\frac{\sin(lk)}{k}$$

and the normalized solution for the vertical displacements in terms of nondimensional quantities

$$\tilde{u}_z = \frac{\pi\mu\omega}{P\beta_3}u_z, \ \ \tilde{U}_z = \frac{\pi\mu\omega}{P\beta_3}U_z, \ \ \tilde{l} = \frac{\omega l}{\beta_3}, \ \ \tilde{x} = \frac{\omega x}{\beta_3}, \ \ \tilde{t} = \omega t$$

can be found as (tildes are omitted):

$$u_z(x,t,\omega) = \mathrm{Re} \int\limits_{-\infty}^{+\infty} \frac{\sin(lp)}{p} \frac{n_2\varsigma_2^2\xi_1(p) - n_1\varsigma_1^2\xi_2(p)}{F(p,\omega)} e^{i(px+t)}dp,$$

$$U_z(x,t,\omega) = -\mathrm{Re} \int\limits_{-\infty}^{+\infty} \frac{\sin(lp)}{p} \frac{1}{F(p,\omega)} n_2\xi_1(p)\left[2p^2(M_1 + M_3) - M_1\right] - $$

$$- n_1\varsigma_1^2\xi_2(p)\left[2p^2(M_2 + M_3) - M_2\right]e^{i(px+t)}dp. \tag{4.40}$$

The above dimensionless solution is represented in the form of a well convergent integrals, as the asymptotic behavior of the integrand amplitude is $\frac{1}{p^2}$ and numerical evaluation does not pose any difficulties. Note, that amplitudes of the displacements will be proportional to the source frequency in the case of the distributed source.

For the practical calculations Fatt's model parameters were used [16]. Figures in Appendix D represent numerical calculations of the integrals (4.37). Non-dimensional time considered is $t = 1$ and the non-dimensional distribution radius is $l = 1/2$ in all cases. Note that this means that the physical radius changes as frequency changes. Depending on the value of the source frequency $\tilde{\omega}$ (4.38) the ocsillatory character of the motion is different. For relatively low frequencies (see Figures D.1, D.2) displacements are in phase, with approximately the same amplitudes, so that further increasing the source frequency leads to weakening of the viscous coupling effect (see Figures D.3, D.4). In this case, when the connection between the phases is less pronounced, solid and fluid displacements can be of different amplitudes and phases (see Figure D.3) or even nearly out of phase (see Figure D.4). The latter case is fairly easy to explain as stress is exerted only on the solid skeleton. As a result of increasing the source frequency values interphase interaction becomes less significant, so that out of phase motion can be observed. It is important to note that the graphs obtained are in agreement with Biot's conclusion [6] that in the range of $\frac{\omega}{\omega_c}$, near unity, the inertia and viscous forces are approximately of the same order. Moreover, the solution obtained in this section is in agreement with the results for solid phase and filtration amplitudes obtained by Valliappan *et al.* in [45] with the application of separation of variables and the fast Fourier transform.

Viscous dissipation in the medium causes attenuation of the signal which is proportional to the distance between the source and observation point. Figures D.5 and D.6 represent solid and fluid phase displacements, respectively, for the typical source frequency values.

4.4 Transient response. Cagniard - de Hoop approach

The transient response forms a far more complicated class of problems in the dynamics of porous media. In the Biot's theory framework problems for a half-space were considered, for example, in [33], [19], [41], [29], [28]. Transient response problems usually lead to the solutions in the form of double Fourier - (or Hankel for axial symmetry) Laplace integrals in the 2D case. Inversion of these integrals is a difficult task from both an analytical and numerical point of view (suffice it to say that Laplace transform inversion is an ill posed problem). For example, in [41], [29] solutions were obtain in Fourier-Laplace space, and transformation to the physical space was suggested only for special limiting cases. Feng and Johnson [19] successfully used the Cagniard - de Hoop approach for investigating high-frequency waves at the fluid/porous media interface. Recent numerical (finite element) studies were presented by Misgoues *et al.* (2005) [28]. In particular, the displacements of the fluid and solid particles over the surface and at depth were studied, as well as, the arrival times of body and surface waves.

The first attempt to obtain an analytic solution in the case of non-dissipative media was carried out by Paul [33]. Using the Diereziewicz [13] potential decomposition an analytical inversion was given by applying the Gakenheimer technique. In Paul's work the following assumptions were made: 1) the P2 wave is faster than the shear wave (S wave), 2) the Rayleigh wave is the slowest. As was shown earlier (see Section 4.2.1, non-dissipative case), the first assumption is not true – for both Fatt's model and Berea sandstone sets of parameters P2 wave is slower than S wave. The second assumption is justified for the Fatt's model, however, the Berea sandstone set of parameters results in a paradoxical situation – non-dissipative surface wave equation has no roots.

The attractive feature of the Cagniard - de Hoop analysis for 2D problems is that exact solutions are possible. Cagniard's approach is based on the application of the Laplace transform and gives the exact solution in the physical time domain. This solution can be further convolved with an arbitrary source function. On the other hand, the disadvantage of this method is that the application of the method

requires certain properties from the Laplace transformed solution. For example, in our particular case we can only consider the case of no dissipation, so that the surface waves are not dispersive. A good discussion of the Cagniard - de Hoop technique, illustrated with practical examples for linear elasticity can be found in [1].

The problem of the transient line traction is considered below for the porous half-space with no dissipation. Unlike the previously mentioned work of Paul, the Cagniard technique will be used (so that no constraints for the relative phase velocities is required) and results will be visualized for two sets of poroelastic parameters: Fatt's model and water saturated Berea sandstone. In the latter case with no dissipation, the Rayleigh equation has no roots. However, it will be demonstrated that this does not mean the complete absence of the surface mode.

Based on the previously obtained general solution (4.29) in the case of the instantaneous line source at the origin we have $P(x) = P\delta(x)$ (4.19), so that $P(k) = \frac{P}{\sqrt{2\pi}}$.

First, as an example, consider the inversion of the P1 component of the vertical solid displacement field $u_z(x, z, s)$:

$$u_z(x, z, s) = -\frac{P}{4\pi\mu} \int_{-\infty}^{+\infty} \frac{\left(2k^2 + \frac{s^2}{\beta_3^2}\right)}{F(k, s)} n_2 \xi_1(k, s) e^{-z \cdot \xi_1(k,s)} e^{ikx} dk. \qquad (4.41)$$

The following change of variable $k = \frac{isp}{\beta_3}$ [1] can be applied in order to obtain the expression, where s is isolated to the argument of the exponential function:

$$u_z(x, z, s) = \frac{P}{4\pi\mu} \int_{-i\infty}^{+i\infty} \frac{i\left(2p^2 - 1\right)}{F(p)} \tilde{n}_2 \varsigma_2^2 \xi_1(p) e^{-\frac{s}{\beta_3}(px + z\xi_1(p))} dp, \qquad (4.42)$$

where $F(p)$ is the Rayleigh wave equation:

$$\begin{aligned} F(p) &= \left(2p^2 - 1\right) \left[\tilde{n}_1 \varsigma_1^2 \left(p^2 - \tilde{m}_2 \varsigma_2^2\right) - \tilde{n}_2 \varsigma_2^2 (p^2 - \tilde{m}_1 \varsigma_1^2)\right] - \\ &\quad - 2p^2 \sqrt{p^2 - 1} \left(\tilde{n}_1 \varsigma_1^2 \sqrt{p^2 - \varsigma_2^2} - \tilde{n}_2 \varsigma_2^2 \sqrt{p^2 - \varsigma_1^2}\right) \end{aligned} \qquad (4.43)$$

and $\xi_{1,2}(p) = \sqrt{p^2 - \varsigma_{1,2}^2}$, $\xi_3(p) = \sqrt{p^2 - 1}$, and $\tilde{n}_{1,2}$, $\tilde{m}_{1,2}$, $\varsigma_{1,2}$ are defined similarly to (4.32), but for the case of no dissipation:
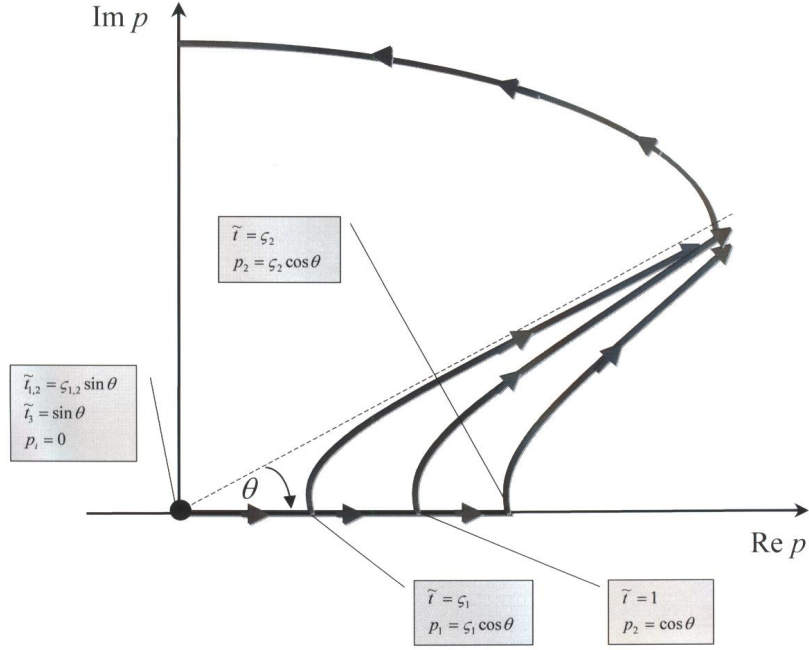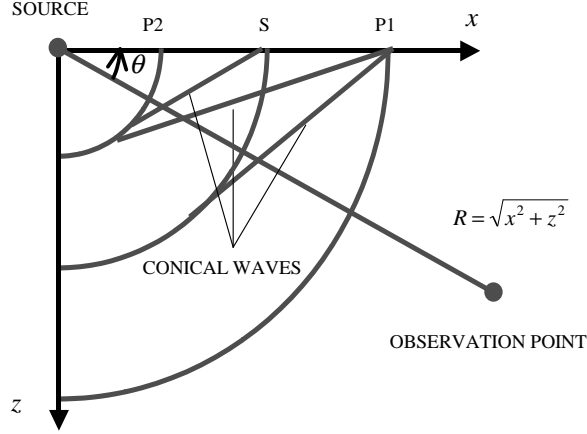
56

Figure 4.6: Cagniard paths in complex p-plane (P1, S and P2)

$$
\begin{aligned}
\varsigma_1 &= \frac{\beta_3}{\beta_2}, \quad \varsigma_2 = \frac{\beta_3}{\beta_1}, \quad \tilde{n}_{1,2} = \frac{Y + RM_{1,2}}{2\mu}, \quad \tilde{m}_{1,2} = \frac{\lambda + 2\mu + YM_{1,2}}{2\mu}, \\
M_{1,2} &= \frac{q_{22}\gamma_{11} - q_{12}\gamma_{12} - (q_{11}q_{22} - q_{12}^2)\bar{z}_{1,2}}{q_{12}\gamma_{22} - q_{22}\gamma_{12}}.
\end{aligned}
$$

Noticing that the real and imaginary parts of $\frac{1}{F(p)}\left(2p^2 - \frac{1}{\beta_3^2}\right)\xi_1(p)e^{-s(px+z\xi_1(p))}$ are even and odd, respectively, for real positive s and purely imaginary values of p one gets

$$
u_z(x,z,s) = -\frac{P}{2\pi\mu}\,\text{Im}\int\limits_{0}^{+i\infty}\frac{(2p^2 - 1)}{F(p)}\tilde{n}_2\varsigma_2^2\xi_1(p)e^{-\frac{s}{\beta_3}(px+\xi_1(p)z)}dp. \tag{4.44}
$$

57

Figure 4.7: Wave fronts and source - receiver angle

Consider an independent variable of integration t, defined as

$$t = \frac{1}{\beta_3} \left[px + \xi_1(p)z \right],$$ (4.45)

so that solving the quadratic equation, p can be expressed as a function of t and one of the roots can be found as

$$p(x, z, t) = \begin{cases} \frac{1}{R^2} \left(x\beta_3 t - z\sqrt{R^2 \varsigma_1^2 - \beta_3^2 t^2} \right) & \text{for} \quad t < \frac{R}{\beta_1} \\ \frac{1}{R^2} \left(x\beta_3 t + iz\sqrt{\beta_3^2 t^2 - R^2 \varsigma_1^2} \right) & \text{for} \quad t > \frac{R}{\beta_1} \end{cases}$$ (4.46)

where $R = \sqrt{x^2 + z^2}$.

The above expression defines the Cagniard path in the complex p plane. It is also easy to show that

$$\frac{dp}{dt} = \frac{i\beta_3 \xi_1(p)}{R\sqrt{\frac{\beta_3^2 t^2}{R^2} - \varsigma_1^2}}.$$ (4.47)

Performing the contour integration along the Cagniard path C (see Figure 4.6) taking into account Jordan's Lemma [1]:

58

$$u_z(x, z, s) = -\frac{P}{2\pi\mu} \operatorname{Im} \oint_C \frac{(2p^2 - 1)}{F(p)} \tilde{n}_2 \varsigma_2^2 \xi_1(p) e^{-\frac{s}{\beta_3}(px + z\xi_1(p))} dp + \sum \operatorname{Res}$$

$$= -\frac{P}{2\pi\mu} \operatorname{Im} \int_{\frac{z}{\beta_1}}^{\infty} \frac{(2p^2 - 1)}{F(p)} \tilde{n}_2 \varsigma_2^2 \xi_1(p) \frac{dp}{dt} e^{-st} dt + \sum \operatorname{Res} \qquad (4.48)$$

and noting that the first term resembles the definition of the Laplace transform, we finally arrive at the following closed form solution:

$$u_z(x, z, t) = -\frac{P}{2\pi\mu} \operatorname{Im} \left\{ \frac{(2p^2 - 1)}{F(p)} \tilde{n}_2 \varsigma_2^2 \xi_1(p) \frac{dp}{dt} H(t - \frac{z}{\beta_1}) \right\}_{p=p(t)} + \sum \operatorname{Res}, \quad (4.49)$$

where $\sum \operatorname{Res}$ denotes the contribution of the residues corresponding to the roots of (4.43) which can possibly be present in the area between the Cagniard path and $\operatorname{Im} p$ axis, or cross the contour.

Introducing non-dimensional time as $\tilde{t} = \frac{\beta_3 t}{R}$ and the source-receiver ray angle θ (see Figure 4.7) the above expression for the non-dimensional slowness (4.46) becomes

$$p(\tilde{t}, \theta) = \begin{cases} \tilde{t} \cos\theta - \sqrt{\varsigma_1^2 - \tilde{t}^2} \sin\theta & \text{for} \quad \tilde{t} < \varsigma_1 \\ \tilde{t} \cos\theta + i\sqrt{\tilde{t}^2 - \varsigma_1^2} \sin\theta & \text{for} \quad \tilde{t} > \varsigma_1 \end{cases} \qquad (4.50)$$

so that the non-dimensional component of the displacement $\tilde{u}_z(\tilde{t}, \theta) = \frac{2\pi\mu R}{P\beta_3} u_z$ (P has a dimension of momentum per unit length) can be expressed as follows:

$$\tilde{u}_z(\tilde{t}, \theta) = -\operatorname{Re} \left\{ \frac{\tilde{n}_2 \varsigma_2^2 (2p^2 - 1)}{F(p)} \frac{\xi_1^2(p)}{\sqrt{\tilde{t}^2 - \varsigma_1^2}} H(\tilde{t} - \varsigma_1 \sin\theta) \right\}_{p=p(\tilde{t}, \theta)} + \sum \operatorname{Res}. \quad (4.51)$$

Proceeding in a similar way, one may obtain closed form solutions for the displacements, components of the stress tensor and pore pressure. Consider, for example, vertical fluid and solid phase displacements (henceforth, tildes over non-dimensional quantities are omitted):

59

$$u_z(t,\theta) = -\mathrm{Re}\left\{\frac{n_2\varsigma_2^2\left(2p_1^2-1\right)}{F(p_1)}\frac{\xi_1^2(p_1)}{\sqrt{t^2-\varsigma_1^2}}H(t-\varsigma_1\sin\theta)\right\}_{p_1=p_1(t,\theta)} +$$

$$+\mathrm{Re}\left\{\frac{n_1\varsigma_1^2\left(2p_2^2-1\right)}{F(p_2)}\frac{\xi_2^2(p_2)}{\sqrt{t^2-\varsigma_2^2}}H(t-\varsigma_2\sin\theta)\right\}_{p_2=p_2(t,\theta)} +$$

$$-\mathrm{Re}\left\{\frac{2p_3^2\left[n_1\varsigma_1^2\xi_2(p_3)-n_2\varsigma_2^2\xi_1(p_3)\right]}{F(p_3)}\frac{\xi_3(p_3)}{\sqrt{t^2-1}}H(t-\sin\theta)\right\}_{p_3=p_3(t,\theta)} +\sum\mathrm{Res},$$

$$U_z(t,\theta) = -\mathrm{Re}\left\{\frac{n_2\varsigma_2^2 M_1\left(2p_1^2-1\right)}{F(p_1)}\frac{\xi_1^2(p_1)}{\sqrt{t^2-\varsigma_1^2}}H(t-\varsigma_1\sin\theta)\right\}_{p_1=p_1(t,\theta)} + \tag{4.52}$$

$$+\mathrm{Re}\left\{\frac{n_1\varsigma_1^2 M_2\left(2p_2^2-1\right)}{F(p_2)}\frac{\xi_2^2(p_2)}{\sqrt{t^2-\varsigma_2^2}}H(t-\varsigma_2\sin\theta)\right\}_{p_2=p_2(t,\theta)} +$$

$$+\mathrm{Re}\left\{\frac{2p_3^2 M_3\left[n_1\varsigma_1^2\xi_2(p_3)-n_2\varsigma_2^2\xi_1(p_3)\right]}{F(p_3)}\frac{\xi_3(p_3)}{\sqrt{t^2-1}}H(t-\sin\theta)\right\}_{p_3=p_3(t,\theta)} +\sum\mathrm{Res},$$

where we have used

$$p_{1,2}(t,\theta)=\begin{cases} t\cos\theta-\sqrt{\varsigma_{1,2}^2-t^2}\sin\theta & \text{for}\quad t<\varsigma_{1,2}\\ t\cos\theta+i\sqrt{t^2-\varsigma_{1,2}^2}\sin\theta & \text{for}\quad t>\varsigma_{1,2}\end{cases}$$

$$p_3(t,\theta)=\begin{cases} t\cos\theta-\sqrt{1-t^2}\sin\theta & \text{for}\quad t<1\\ t\cos\theta+i\sqrt{t^2-1}\sin\theta & \text{for}\quad t>1\end{cases}$$

$$M_{1,2}=\frac{q_{22}\gamma_{11}-q_{12}\gamma_{12}-(q_{11}q_{22}-q_{12}^2)\bar{z}_{1,2}}{q_{12}\gamma_{22}-q_{22}\gamma_{12}},\qquad M_3=\frac{\gamma_{12}}{\gamma_{22}}.$$

In Appendix E (Fatt's model) and Appendix F (water saturated Berea sandstone) numerical results in accordance with (4.52) are presented for different observation angles in the range $0<\theta<\frac{\pi}{2}$, so that $\theta=0$ corresponds to the displacements calculated at the surface, while $\theta=\frac{\pi}{2}$ corresponds to the case when the observation point is located directly below the source (red and blue lines correspond to solid and fluid phase displacements, respectively). The obtained solution scales in the

following way: non-dimensional quantities ς_1 and ς_2 represent nondimensional wave front arrival times for the P1 and P2 waves respectively, while the non dimensional arrival time for the shear wave is $t = 1$.

Figure 4.8 represents a typical result obtained in accordance with (4.52) for the Berea sandstone set of parameters. In this case one can observe the following sequence of the wave fronts arrivals: P1, S, Rayleigh and P2-wave. Integrable singularities at the arrival times for the head waves (P1, P2, S) are caused by the Dirac function time dependence of the loading and would disappear if the smooth function was considered instead, for the instantly starting loading. Conical waves can also be observed as a consequence of the energy radiation of the P1-wave into S and P2 motions, and of S-wave into P2 motion (see Figure 4.7).
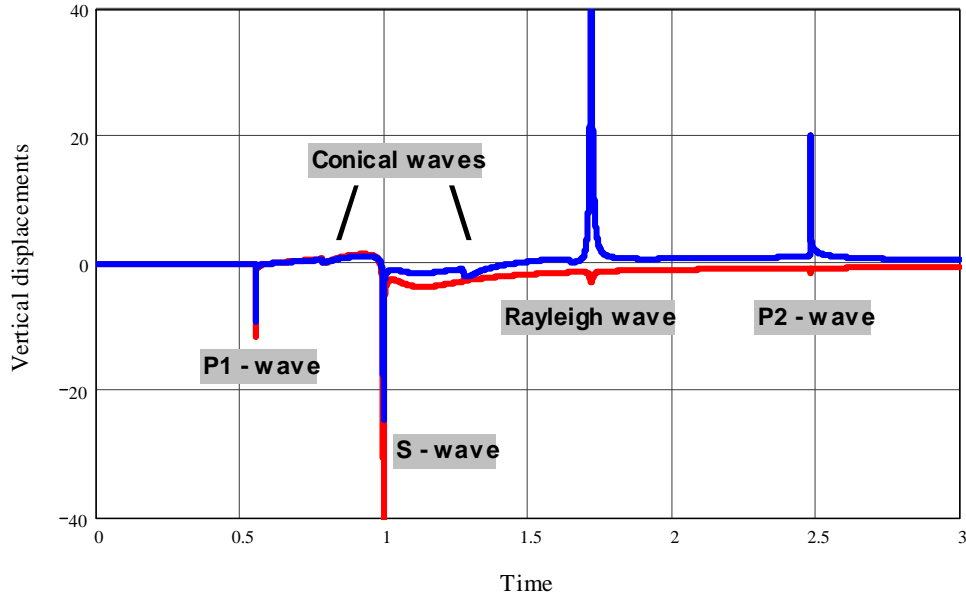
Figure 4.8: Typical wave picture (water saturated Berea sandstone, source - receiver angle $\theta = \frac{\pi}{10}$)

As was mentioned above, the assumption made by Paul in [33] that the Rayleigh wave is slower than all three head waves (including P2) is not always true for a non dissipative case. For instance, it can be demonstrated that while this assumption is justified for the Fatt's model, other possibilities may arise, for example, in the case of the water saturated Berea sandstone. The results for the nondimensional wave front arrival times are summarized in the table below (p_R is the root of the

Rayleigh equation (4.43))

Material	$\varsigma_1 = \frac{\beta_3}{\beta_1}$	$\varsigma_2 = \frac{\beta_3}{\beta_2}$	p_R
Fatt's model	0.509	1.101	1.1027
Water saturated berea sandstone	0.556	2.484	no root

In the case of the water saturated Berea sandstone the Rayleigh wave equation has no roots, however, this does not imply that a surface mode disappears. Mathematically, there is a certain value of p such that in the vicinity of this point, the Rayleigh waves equation (4.43) takes values close to zero. As the denominator of the function evaluated along the Cagniard is close to zero, one can observe the surface wave inspite of the fact that secular equation has no roots. In this special case one can observe the radiation of the surface wave energy below the surface into the fluid phase. The surface mode is well pronounced in the interior until its velocity becomes close to the P2 wave velocity, afterwards it is no longer propagating.

Finally, it should be mentioned, that the solution obtained agrees with physical expectations: first of all, there is no motion observed faster than the P1 wave; second, the solution for the displacements vanishes as $t \to \infty$ (which is the only possibility for Dirac type loading); finally, the solution obtained is in agreement with the Biot's conclusion [6] (see orthogonality relation) that out of phase motion is expected in the P2 wave. Amplitudes of a different sign are clearly visible in the case of the Berea sandstone graphs (Appendix F).

Chapter 5

Conclusions

5.1   Summary

Two main mathematical models of porous media were considered: consolidation theory (quasi-static) and Biot's theory (dynamic). In particular, it was demonstrated that 1D consolidation problems for a semi infinite domain allow simple analytic solutions (permeable piston problem, creep problem, liquid piston problem), however, the main focus was on the wave propagation problems in the framework of Biot's theory. Solutions for 2D problems for a porous half-space with steady state and transient (for the inviscid case) line tractions were obtained and analyzed.

Mathematical methods used included application of the Helmholtz potential decomposition, in order to decompose Biot's set of equations into elementary wave motions of dilatational (P1, slow P2) and solenoidal (shear S) type. The general solution for normal surface traction was found in Laplace - Fourier space. Results in physical space for the Fatt's model (kerosene saturated sandstone) and water saturated Berea sandstone were discussed for both the steady state case (via numerical inversion of the Fourier transform) and the transient case (using the Cagniard de Hoop technique).

5.2   Conclusions

The main results mostly concern the wave propagation issues and can be subdivided into three parts: the conclusions regarding the surface wave propagation in dissipative and non-dissipative media, the results for a steady-state response, and, finally, the results for the transient response.

Surface waves

Results obtained for the phase velocities and attenuations of the surface wave agree with the results obtained in early work by Deresiewicz [13] for the dissipative medium and with [41] for the case of no dissipation.

It was shown that when dissipation effects are included, the surface wave is always attenuated and, therefore, will be less pronounced. The velocity of propagation of this wave may be determined for all frequencies ω between 0 and ∞. The velocity is always smaller than the phase velocity of the shear S-wave. As a function of ω, it possesses an inflection point and is slightly non-monotonic in the range of small frequencies (i.e. possesses a weak minimum). The attenuation of this wave grows from zero for $\omega \to 0$ and reaches a maximum, then monotonically decays for larger ω so that $\omega \to \infty$ will give zero attenuation. This demonstrates a significant difference between the two cases: namely that dispersive surface waves may propagate either faster (high frequency range) or slower (low frequency range), compared to non dispersive ones. For example, the phase velocity of the surface wave in the Fatt's model varies in the following range: $\approx 317.6\frac{m}{s} - 328.5\frac{m}{s}$, while the non dissipative propagation speed was determined as $\approx 326.262\frac{m}{s}$.

It is also demonstrated that the dispersion equation of the surface waves may not have any roots (Berea sandstone) in the case of no dissipation, however, this does not imply the absence of the surface mode (see results for the transient response).

In summary, the main conclusion, justified with two sets of parameters is: while phase velocity and attenuation is observed to rise with increasing frequencies for P1, P2 and S wave motion (see [6], [9]) Rayleigh wave propagation speed and attenuation are non monotonic.

Steady state response

Solutions for the steady-state line traction were obtained in the form of slowly decaying highly oscillating integrals. The possibilities of numerical integration were discussed. Numerical results were presented for the following two cases: line source (Green's function) and uniformly distributed source. Unlike previous studies (for example, [23], [45]), the main focus in the present work was on the response at a different source frequencies. It was demonstrated that depending on the value of the source frequency the character of spatial ocsillations of the motion is different. For relatively low frequencies displacements were observed to be in phase, with approximately the same amplitudes. Increasing the source frequency led to a weakening of the viscous coupling effect and, as a consequence, solid and fluid

displacements could be of different amplitudes and phases, or in fact nearly out of phase in the high frequency range. The numerical results were in agreement with Biot's conclusion [6] that in the range of the characteristic frequency near unity, the inertia and viscous forces are approximately of the same order. Moreover, the presented solution was in agreement with the results for solid phase and filtration amplitudes obtained by Valliappan *et al.* in [45] with the application of separation of variables and the fast Fourier transform.

Finally, unlike the results for a similar axially symmetric problem with a point source, reported by Halpern and Christiano in [23] (divergent integrals for the vertical displacements), the expression for the exact Green's function was obtained and numerical results presented for both Fatt's model and water saturated Berea sandstone.

Transient response

A beginning, along the lines of the present study, was made by Paul [33], where analytic solution of the Lamb's problem for a non-dissipative medium with a free surface pressure was obtained based on the Cagniard - de Hoop technique modified by Gakenheimer. One of the assumptions made in [33] that the P2 wave is faster than the S wave, appears not to be justified for most materials observed in nature. Moreover, no graphical information was presented in [33].

Unlike the above mentioned study, the analytical solution obtained in the present work does not require any constraints on the relative head wave phase velocities. The solution for the solid and fluid phase displacements at the surface, as well as in the interior, was visualized for two typical sets of parameters – Fatt's model and Berea sandstone. The presented solution agrees with physical expectations: first of all, there is no motion observed that is faster than the P1 wave; second, the solution for the displacements vanishes as $t \to \infty$ (which is the only possibility for Dirac type loading); finally, the solution obtained is in agreement with Biot's conclusion [6] that motion in the P2 wave is out of phase: amplitudes of different signs are clearly visible in the case of the Berea sandstone graphs (Appendix F).

The presented solution clearly exhibits the following sequence of wave front arrivals: P1, S, Rayleigh and P2-wave Integrable singularities at the arrival times for the head waves (P1, P2, S) are caused by the Dirac function time dependence of the loading and would disappear in the case of a smooth source function for the loading. In addition, conical waves can also be observed as a consequence of the energy radiation from the P1-wave into S and P2 motions, and from the S-wave into P2 motion. In particular, it is demonstrated that in the case of the water

65

saturated Berea sandstone even though the Rayleigh wave equation has no roots, a free surface mode is apparent. In this special case one can observe the radiation of the surface wave energy below the surface into the fluid phase: the surface mode is well pronounced in the interior until its velocity becomes close to the P2 wave velocity, afterwards it is no longer propagating.

5.3 Future work

Studies of the wave processes in porous media are motivated mostly by the applications in the field of the seismic prospecting in petrophysics and nondestructive testing. For example, low-frequency seismic prospecting (around $50Hz$) is intended to detect and analyze interesting geological horizons under sediment thicknesses up to several kilometers. High frequency prospecting or acoustic logging ($\approx 10^4 Hz$) is used for measurements in wells, directed at the particular beds of interest. A higher range of signal frequencies ($> 10^6 Hz$) is of interest in the area of nondestructive testing of systems such as soils and rocks, concrete, asphalt and other porous construction materials, bones and soft tissues such as the surface of the heart, and surface coating by nanomaterials. Medical applications allow for frequencies up to approximately $3MHz$ while testing of nanomaterials requires frequencies of approximately $100MHz$.

Further studies of the wave propagation in porous materials can be conducted not only for the Biot's theory framework, but also for Wilmanski's theory [48] and TPM [12]. Especially, for the latter two theories wave propagation is mostly *terra incognita*. No boundary problems have been solved, to date, however, some results regarding surface waves were obtained, see for instance [2], [27], [12]. Problems for a layered medium (except porous/fluid interface) are not covered in the literature, for example – wave propagation along the plane interface between two porous materials with different mechanical properties, or waves on a porous / perfectly elastic interface, as well as problems with internal sources. We hope to examine some of these problems in the future.

Appendix A

Coefficients for characteristic equation

It is known that for a 2x2 matrix $\|a_{ij}\|$, the eigenvalues arise as the solutions of the characteristics equation:

$$z^2 - (a_{11} + a_{22})z + \det\|a_{ij}\| = 0.$$

If components are given by (4.6), expression for $a_{11} + a_{22}$ becomes:

$$
\begin{aligned}
a_{11} + a_{22} &= q_{22}\gamma_{11} - q_{12}\gamma_{12} + (q_{22} + q_{12})b/\rho s - q_{12}\gamma_{12} + q_{11}\gamma_{22} + (q_{12} + q_{11})b/\rho s \\
&= q_{11}\gamma_{22} + q_{22}\gamma_{11} - 2q_{12}\gamma_{12} + (q_{11} + 2q_{12} + q_{22})b/\rho s \\
&= q_{11}\gamma_{22} + q_{22}\gamma_{11} - 2q_{12}\gamma_{12} + b/\rho s,
\end{aligned}
$$

here obvious identity $q_{11} + 2q_{12} + q_{22} = 1$ is used.

Expression for $\det\|a_{ij}\|$ becomes:

$$
\begin{aligned}
\det\|a_{ij}\| = {}& -q_{12}q_{22}\gamma_{11}\gamma_{12} + q_{11}q_{22}\gamma_{11}\gamma_{12} + q_{22}\gamma_{11}(q_{11} + q_{12})b/\rho s + \\
& +q_{12}^2\gamma_{12}^2 - q_{11}q_{12}\gamma_{12}\gamma_{22} - q_{12}\gamma_{12}(q_{11} + q_{12})b/\rho s - \\
& -q_{12}\gamma_{12}(q_{12} + q_{22})b/\rho s + q_{11}\gamma_{22}(q_{22} + q_{12})b/\rho s + \\
& +q_{12}q_{22}\gamma_{11}\gamma_{12} - q_{11}\gamma_{22}\gamma_{12}^2 + q_{22}\gamma_{12}(q_{11} + q_{12})b/\rho s - \\
& -q_{12}^2\gamma_{11}\gamma_{22} + q_{11}q_{12}\gamma_{12}\gamma_{22} - q_{12}\gamma_{22}(q_{11} + q_{12})b/\rho s - \\
& -q_{12}\gamma_{11}(q_{12} + q_{12})b/\rho s + q_{11}\gamma_{12}(q_{22} + q_{12})b/\rho s.
\end{aligned}
$$

Simplifying the above expression one can get:

$$
\begin{aligned}
\det \|a_{ij}\| &= q_{11}q_{22}\gamma_{11}\gamma_{12} + q_{12}^2\gamma_{12}^2 - q_{12}^2\gamma_{11}\gamma_{22} - q_{11}\gamma_{22}\gamma_{12}^2 + \\
&\quad + b/\rho s(q_{22}\gamma_{11}q_{11} - 2q_{12}^2\gamma_{12} + q_{11}q_{22}\gamma_{22} - q_{12}^2\gamma_{11} + q_{12}^2\gamma_{11} + 2q_{11}q_{22}\gamma_{12} - q_{12}^2\gamma_{22}) \\
&= (q_{11}q_{22} - q_{12}^2)\left[(\gamma_{11}\gamma_{12} - \gamma_{12}^2) + b/\rho s(\gamma_{11} + 2\gamma_{12} + \gamma_{22})\right] \\
&= (q_{11}q_{22} - q_{12}^2)\left[(\gamma_{11}\gamma_{12} - \gamma_{12}^2) + b/\rho s\right].
\end{aligned}
$$

Appendix B

Dispersion polynomial coefficients

Coefficients A_i for the polynomial

$$D(p) = \sum_{n=0}^{8} A_n p^n$$

corresponding to the no dissipation Rayleigh waves dispersion relation:

$A_0 = 1$

$A_1 = -16$

$A_2 = -32(K_1^2 \zeta_2^2 + K_2^2 \zeta_1^2) + 112$

$A_3 = 288(K_1^2 \zeta_2^2 + K_2^2 \zeta_1^2) + 32(K_1^2 + K_2^2) - 448$

$A_4 = -512K_1^2 K_2^2 \zeta_2^2 \zeta_1^2 + 256(K_1^4 \zeta_2^4 + K_2^4 \zeta_1^4) - 1024(K_1^2 \zeta_2^2 + K_2^2 \zeta_1^2) -$

$-288(K_1^2 + K_2^2) + 1120$

$A_5 = 1024K_1^2 K_2^2 \zeta_2^2 \zeta_1^2 - 512(K_1^4 \zeta_2^4 + K_2^2 \zeta_1^4) - 512(K_1^4 \zeta_2^2 + K_2^4 \zeta_1^2) +$

$+512K_1^2 K_2^2 (\zeta_2^2 + \zeta_1^2) + 1792(K_1^2 \zeta_2^2 + K_2^2 \zeta_1^2) + 1024(K_1^2 + K_2^2) - 1792$

$A_6 = -512K_1^2 K_2^2 \zeta_2^2 \zeta_1^2 - 1024K_1^2 K_2^2 (\zeta_2^2 + \zeta_1^2) + 256(K_1^4 \zeta_2^4 + K_2^4 \zeta_1^4) +$

$+1024(K_1^4 \zeta_2^2 + K_2^2 \zeta_1^2) - 1536(K_1^2 \zeta_2^2 + K_2^2 \zeta_1^2) + 256(K_1^4 + K_2^4) -$

$-512K_1^2 K_2^2 - 1792(K_1^2 + K_2^2) + 1792$

$A_7 = 512K_1^2 K_2^2 (\zeta_2^2 + \zeta_1^2) - 512(K_1^4 \zeta_2^2 + K_2^2 \zeta_1^2) + 512(K_1^2 \zeta_2^2 + K_2^2 \zeta_1^2) -$

$-512(K_1^4 + K_2^4) + 1536(K_1^2 + K_2^2) + 1024K_1^2 K_2^2 - 1024$

$A_8 = 256(K_1^4 + K_2^4) - 512(K_1^2 + K_1^2 K_2^2 + K_2^2) + 256 = 0$

Appendix C

Exact Green's functions. Fatt's model
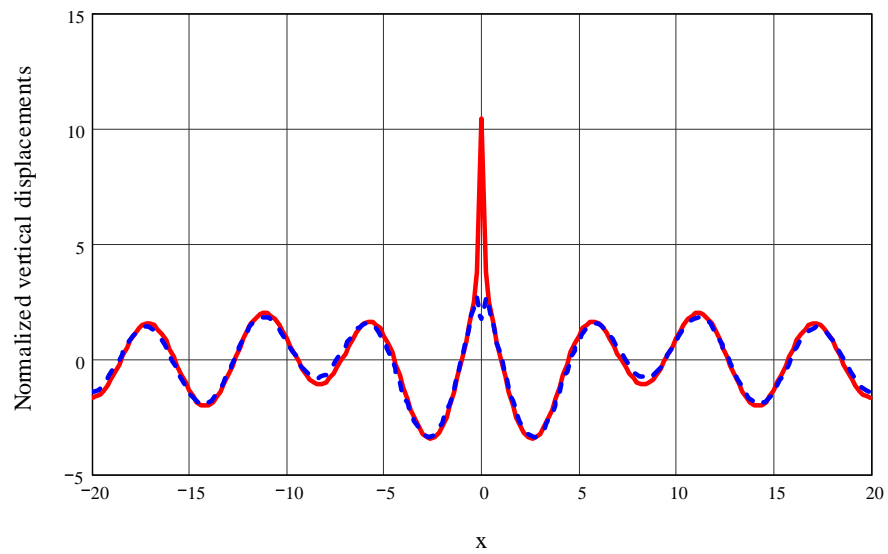
Figure C.1: Fatt's model Green function. Source frequency $w = 0.1w_c$
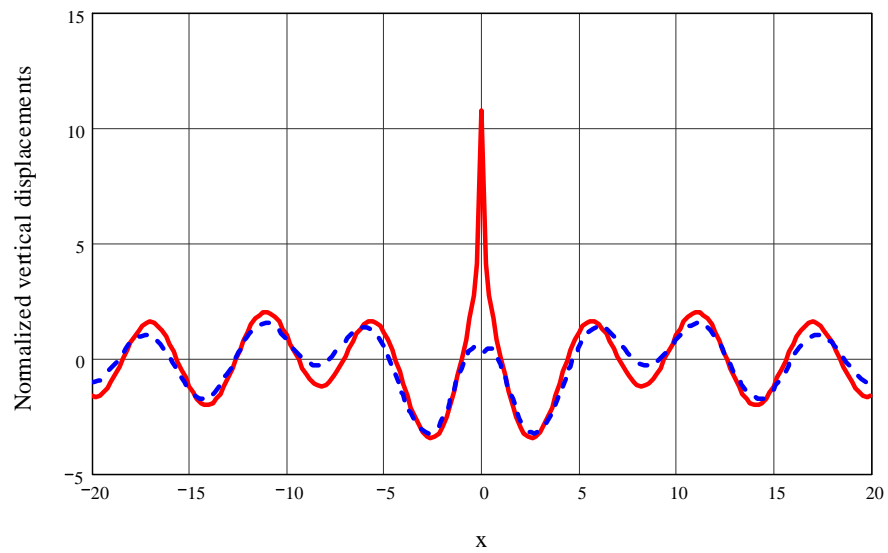
Figure C.2: Fatt's model Green function. Source frequency $w = w_c$
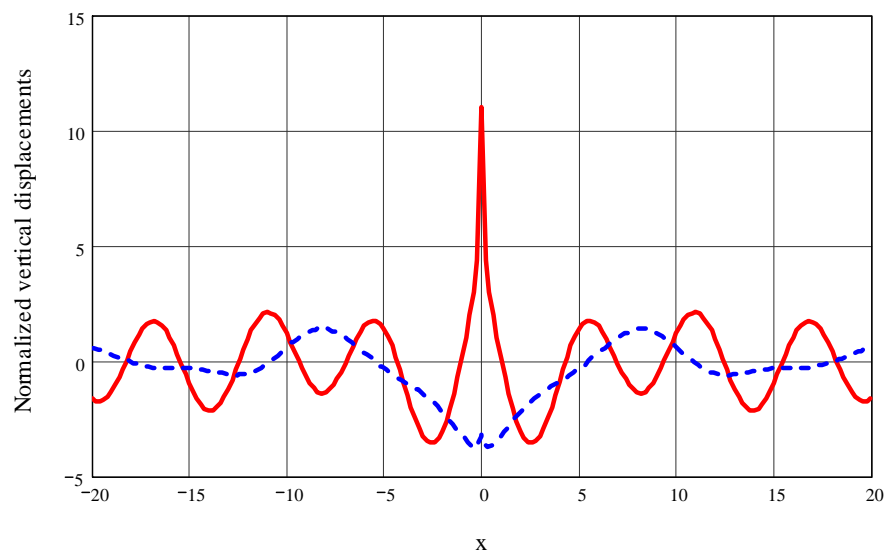
Figure C.3: Fatt's model Green function. Source frequency $w = 10w_c$
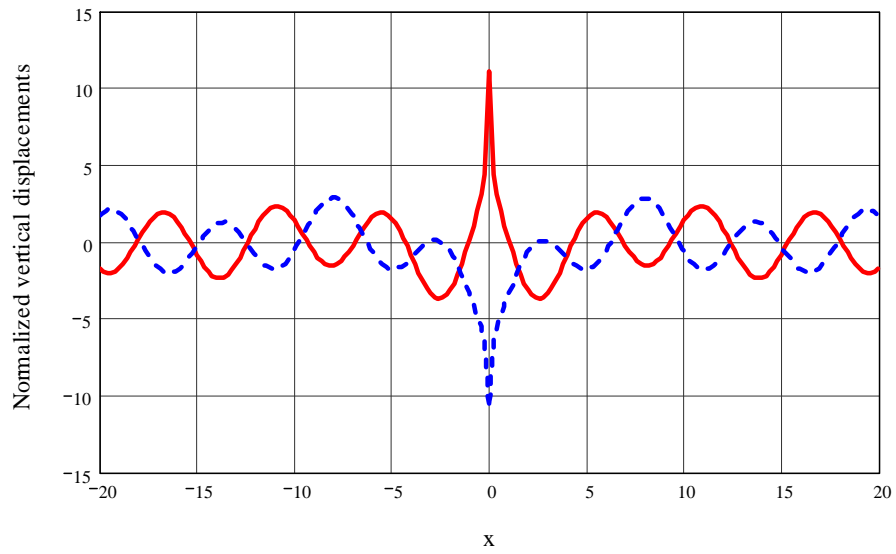
Figure C.4: Fatt's model Green function. Source frequency $w = 100w_c$

Appendix D

Uniformly distributed source. Fatt's model
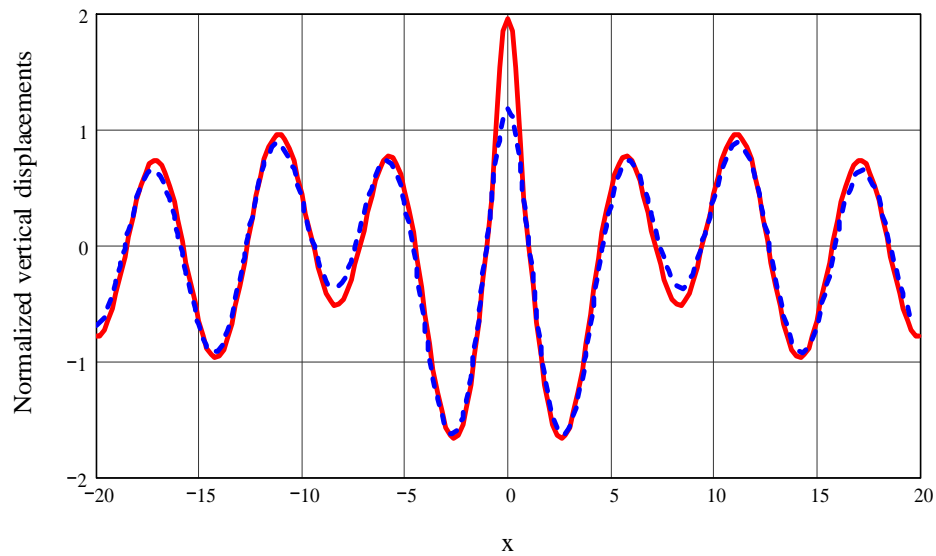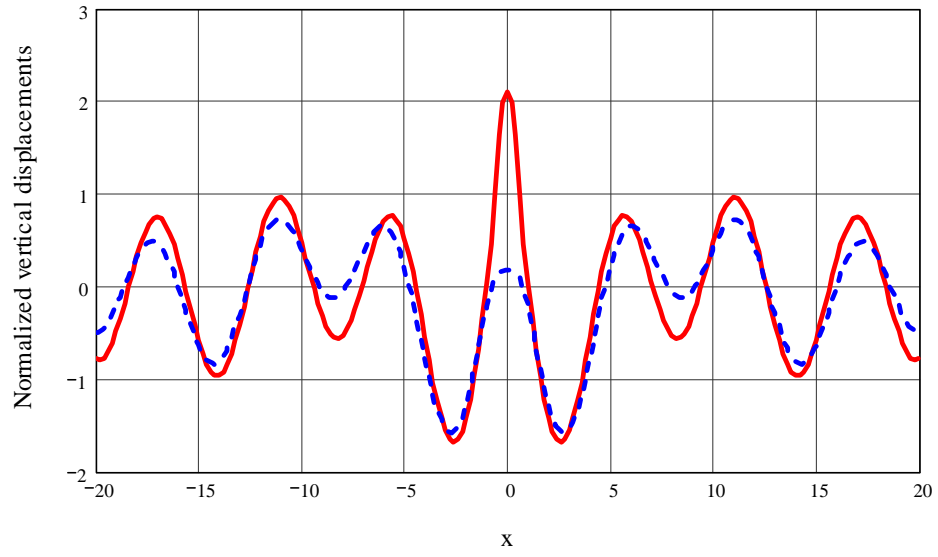

Figure D.1: Fatt's model. Source frequency $w = 0.1w_c$

Figure D.2: Fatt's model. Source frequency $w = w_c$
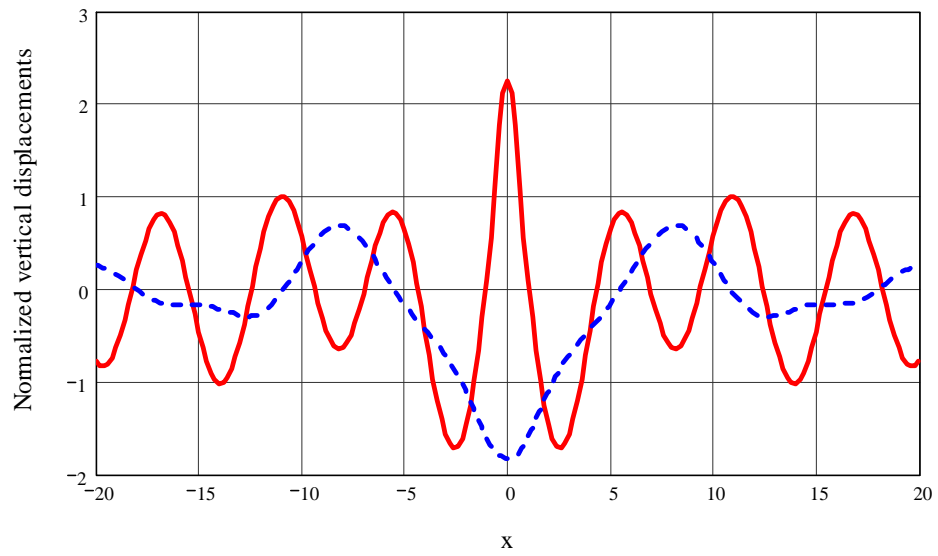
Figure D.3: Fatt's model. Source frequency $w = 10w_c$
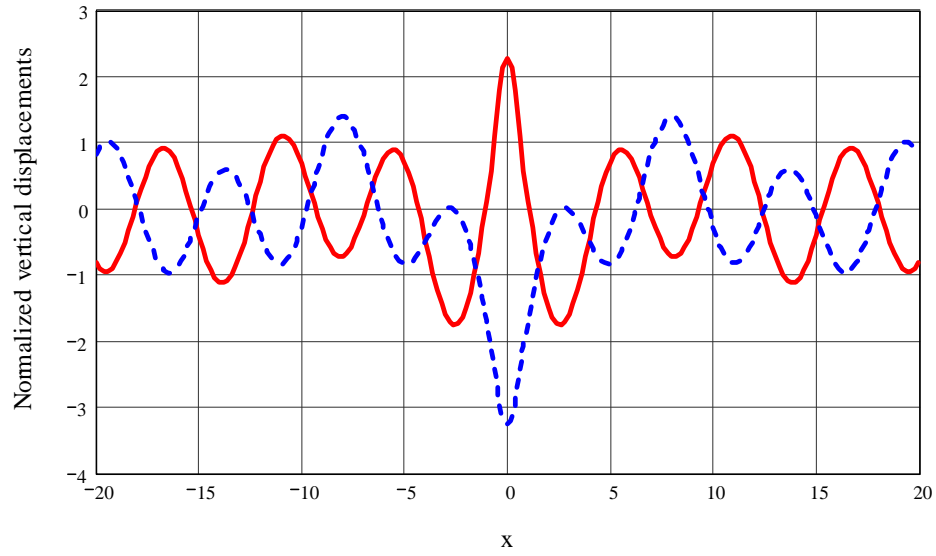
Figure D.4: Fatt's model. Source frequency $w = 100w_c$
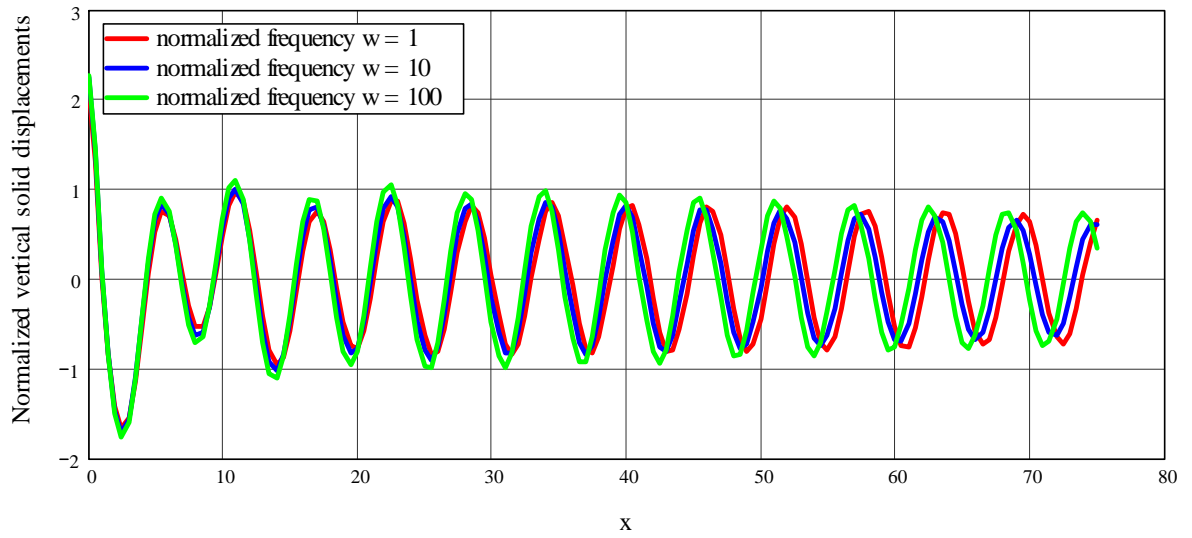
Figure D.5: Fatt's model. Solid phase displacements. Source frequencies: $w = w_c$, $w = 10w_c$, $w = 100w_c$
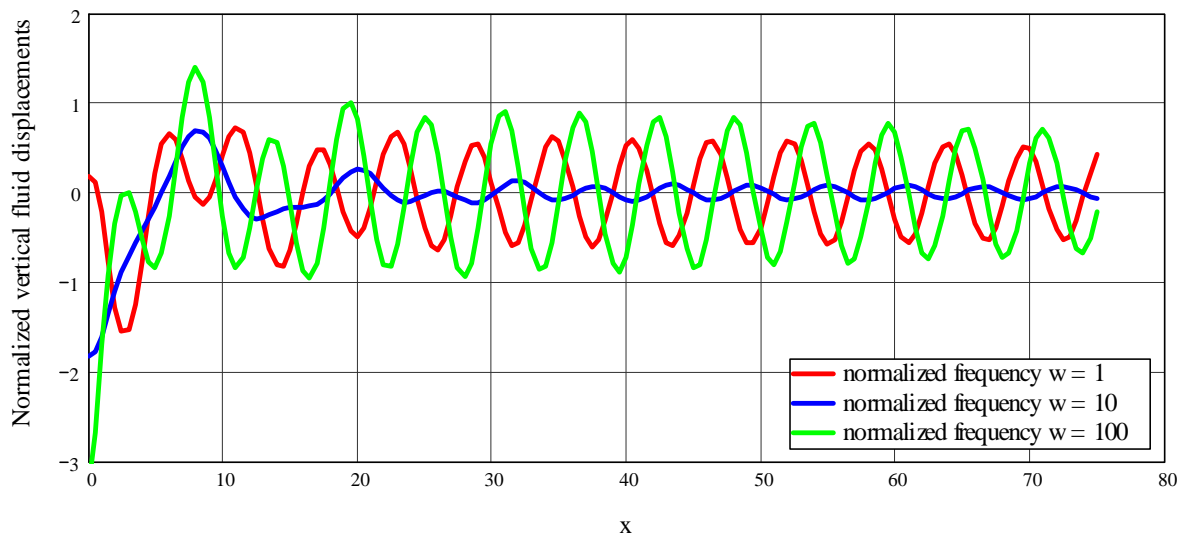
Figure D.6: Fatt's model. Fluid phase displacements. Source frequencies: $w = w_c$, $w = 10w_c$, $w = 100w_c$

Appendix E

Transient response. Fatt's model
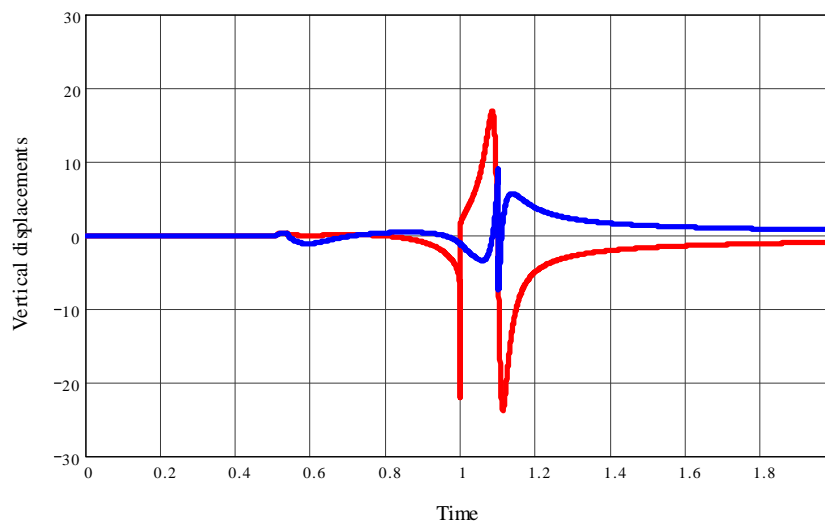
Figure E.1: Fatt's model. Source - receiver angle $\theta = \frac{\pi}{100}$
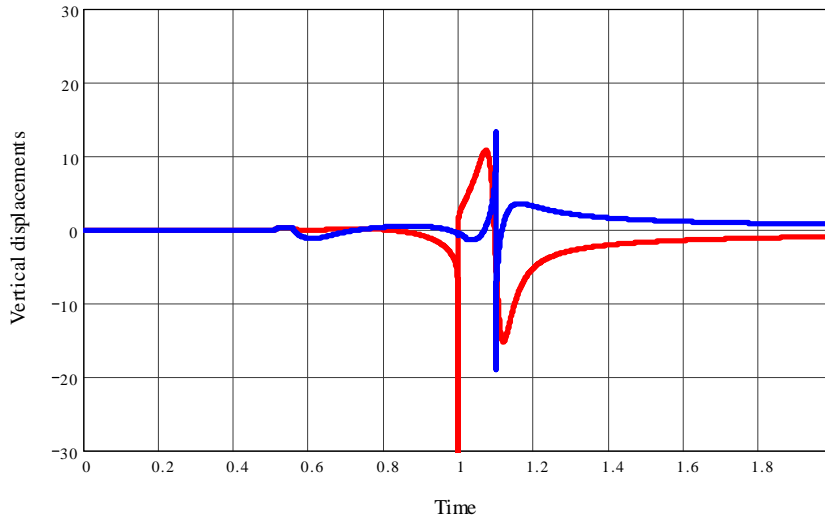
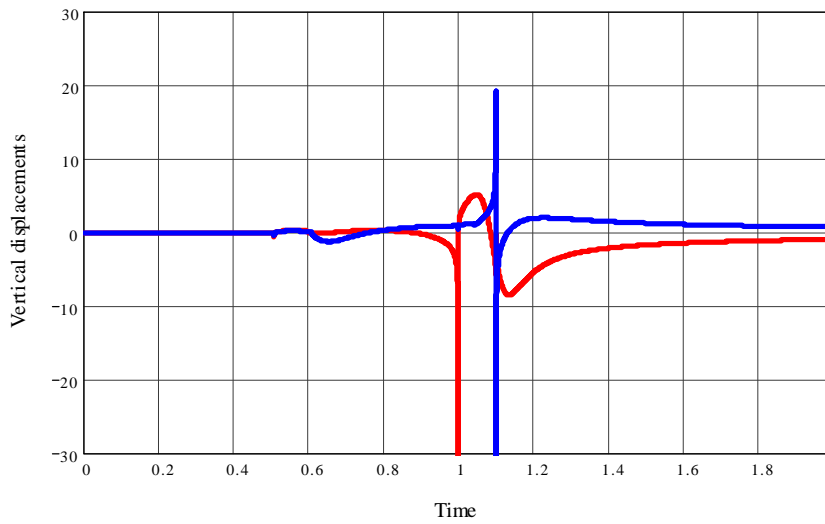Figure E.2: Fatt's model. Source - receiver angle $\theta = \frac{\pi}{60}$

Figure E.3: Fatt's model. Source - receiver angle $\theta = \frac{\pi}{30}$
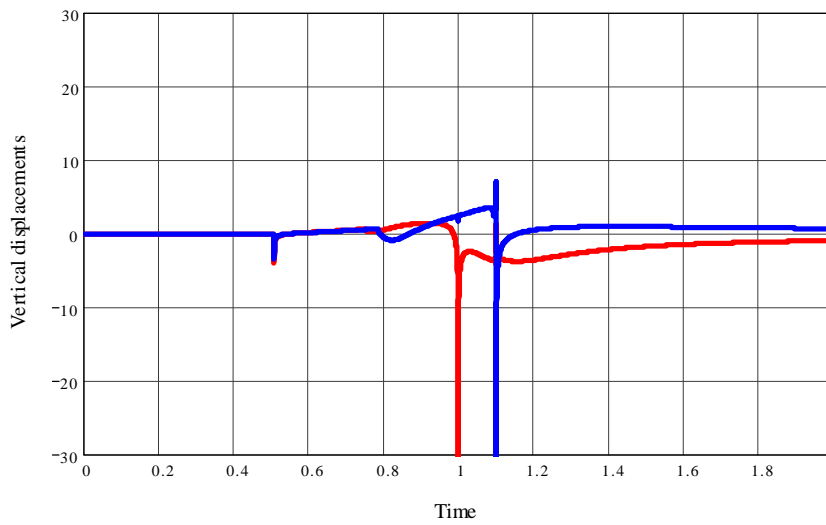
Figure E.4: Fatt's model. Source - receiver angle $\theta = \frac{\pi}{10}$

Appendix F

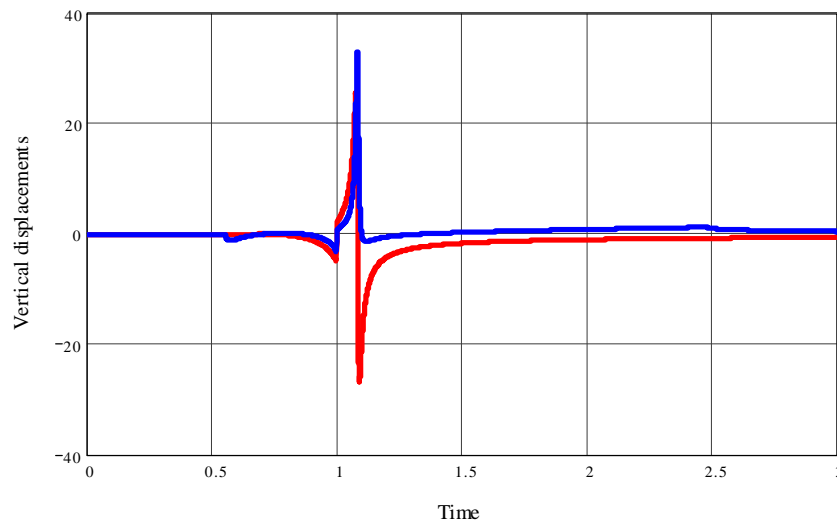# Transient response. Water saturated Berea sandstone

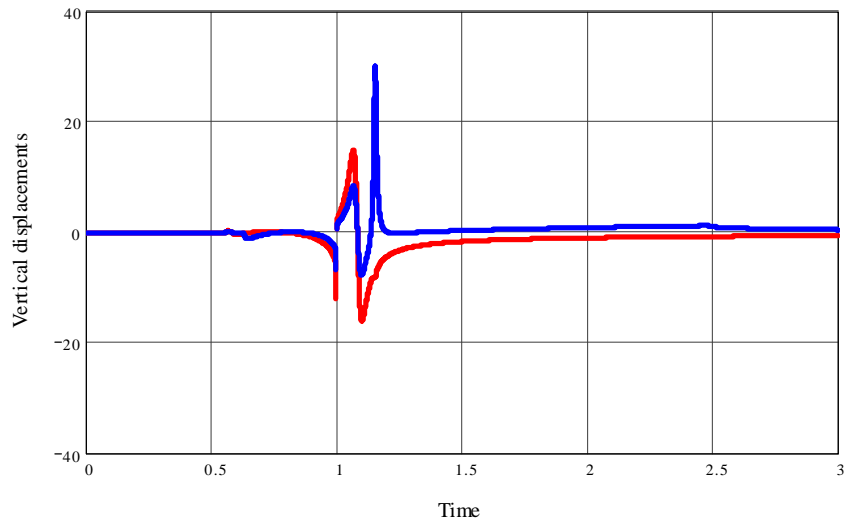Figure F.1: Water saturated Berea sandstone. Source - receiver angle $\theta = 0$

Figure F.2: Water saturated Berea sandstone. Source - receiver angle $\theta = \frac{\pi}{100}$
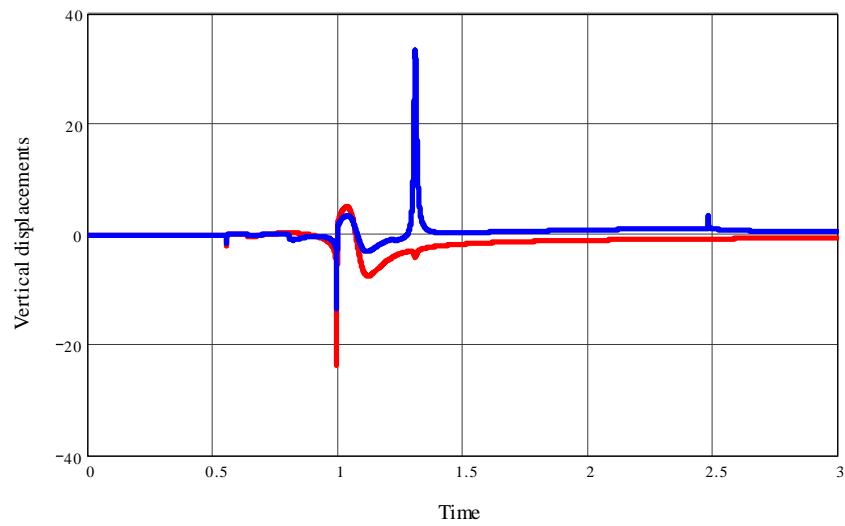

Figure F.3: Water saturated Berea sandstone. Source - receiver angle $\theta = \frac{\pi}{30}$

81

Figure F.4: Water saturated Berea sandstone. Source - receiver angle $\theta = \frac{\pi}{10}$

Figure F.5: Water saturated Berea sandstone. Source - receiver angle $\theta = \frac{\pi}{6}$

82
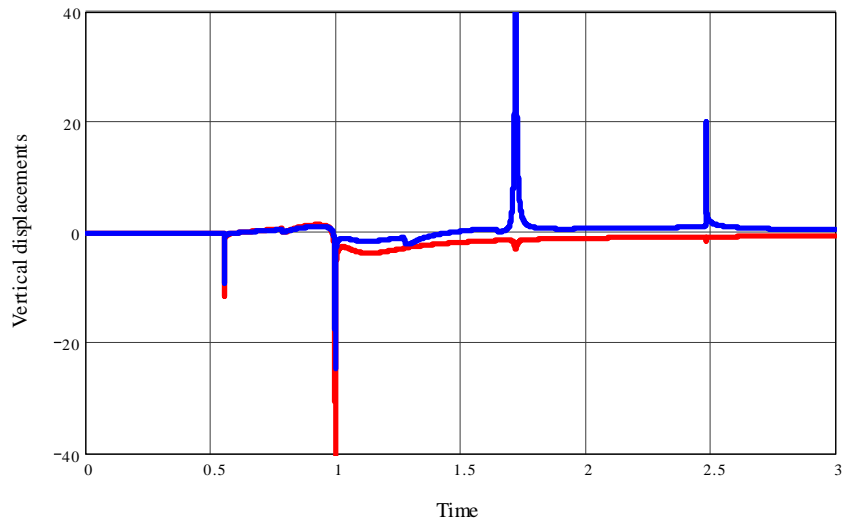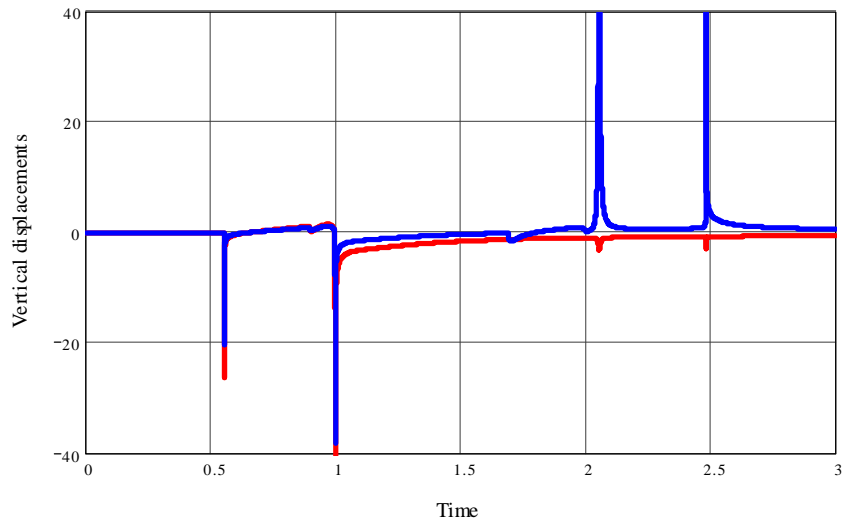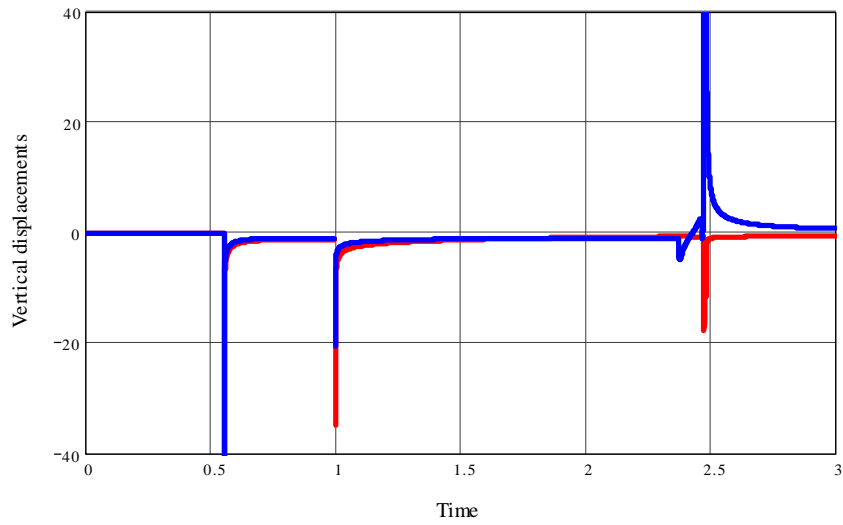
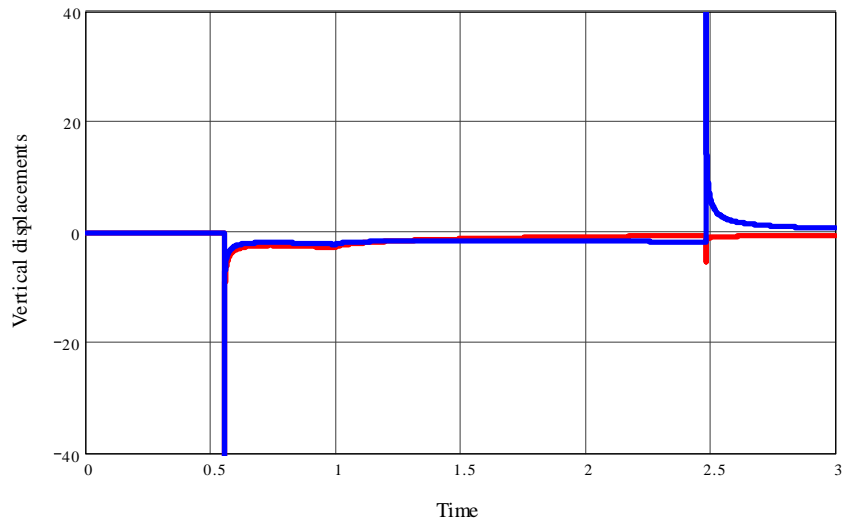Figure F.6: Water saturated Berea sandstone. Source - receiver angle $\theta = \frac{\pi}{3}$

Figure F.7: Water saturated Berea sandstone. Source - receiver angle $\theta = \frac{\pi}{2}$

Appendix G

Physical properties of the porous materials used in calculations

G.1 Kerosene saturated sandstone

(referred as "Fatt's model", see [16], [41])

$$
\begin{aligned}
\lambda &= 0.4026 \cdot 10^9 \frac{kg}{ms^2}, & \mu &= 0.2493 \cdot 10^9 \frac{kg}{ms^2}, \\
Y &= 0.0672 \cdot 10^9 \frac{kg}{ms^2}, & R &= 0.0295 \cdot 10^9 \frac{kg}{ms^2}.
\end{aligned}
$$

Porosity:

$$\phi = 0.26\%.$$

Permeability:

$$k = 100 mD.$$

Solid grains and pore fluid densities:

$$
\rho_f = 0.82 \cdot 10^3 \frac{kg}{m^3}, \qquad \rho_s = 2.6 \cdot 10^3 \frac{kg}{m^3}.
$$

Reference phase densities (mass matrix $\tilde{M}$):

$$\tilde{M} = \begin{pmatrix} \rho_{11} & \rho_{12} \\ \rho_{12} & \rho_{22} \end{pmatrix} = \begin{pmatrix} 1.9259 & -0.0019 \\ -0.0019 & 0.2151 \end{pmatrix} \cdot 10^3 \frac{kg}{m^3}.$$

G.2 Berea sandstone and the saturating fluids: water and air

(referred as "Berea sandstone", see [42], [11])

Porosity	ϕ	0.20
Permeability (mD)	k	360
Tortuosity	a	2.4
Frame bulk modulus (GPa)	K_b	10.37
Shear modulus (GPa)	μ	7.02
Grain bulk modulus (GPa)	K_s	36.5
Liquid bulk modulus (GPa)	K_f	2.25
Gas pressure (bulk modulus) (GPa)	K_g	0.01
Solid density (kg/m^3)	ρ_s	2644
Liquid density (kg/m^3)	ρ_f	1000
Gas density (kg/m^3)	ρ_g	100
Liquid viscosity $(mPa\ s)$	η_f	1
Gas viscosity $(mPa\ s)$	η_g	0.015

For example, in the water saturation case, Biot's poroelastic coefficients and reference densities can be found in accordance with (2.25) as

$$\begin{aligned} \lambda &= 7.564 \cdot 10^9 \frac{kg}{ms^2}, & \mu &= 7.02 \cdot 10^9 \frac{kg}{ms^2}, \\ Y &= 0.726 \cdot 10^9 \frac{kg}{ms^2}, & R &= 0.282 \cdot 10^9 \frac{kg}{ms^2}. \end{aligned}$$

Reference phase densities (mass matrix $\tilde{M}$):

$$\tilde{M} = \begin{pmatrix} \rho_{11} & \rho_{12} \\ \rho_{12} & \rho_{22} \end{pmatrix} = \begin{pmatrix} 2.395 & -0.28 \\ -0.28 & 0.480 \end{pmatrix} \cdot 10^3 \frac{kg}{m^3}.$$

Bibliography

[1] Aki K., Richards P., "*Quantitative seismology. Theory and methods*", W.H. Freeman and company, San-Francisco, 1980.

[2] Albers B., Wilmanski K., "Monochromatic surface waves on impermeable boundaries in two-component poroelastic media", *Continuum Mech. Thermodyn.*, 17, 269–285, 2005.

[3] Berryman, J.G., "Confirmation of Biot's theory", *Appl. Phys. Lett.*, 37, 382-384, 1980.

[4] Biot M.A., "General theory of three-dimensional consolidation", *J. Appl. Phys.*, 155-164, 1941.

[5] Biot, M.A., "Theory of elasticity and consolidation for a porous anisotropic solid", *J. Appl. Phys.*, 26, 182-185, 1955.

[6] Biot, M.A., "The theory of propagation of elastic waves in a fluid-saturated porous solid", *J. Acous. Soc. Amer.*, 28, 168-191, 1956.

[7] Biot M.A., "Mechanics of deformation and acoustic propagation in porous media", *J. Appl. Phys.*, 23, 1482-1498, 1962.

[8] Bonnet G., "Basic singular solutions for a poroelastic medium in the dynamic range", *J. Acoust. Soc. Amer.*, 82, 1758-1762, 1987.

[9] Bourbie T., Coussy O., Zinzner B., "*Acoustics of porous media*", Gulf publishing company, Paris, 1987.

[10] Brinkman H.C., "A calculation of the viscous force exerted by a flowing fluid on a dense swarm of particles", *Appl. Scientific Res.*, 1, 769-790, 1957.

[11] Chao G., Smeulders D. M. J., van Dongen M. E. H., "Dispersive surface waves along partially saturated porous media", *J. Acous. Soc. Amer.*, 119, 1348-1355, 2006.

[12] de Boer R., "*Trends in continuum mechanics of porous media*", Springer, 2005.

[13] Deresiewicz H., Rice J.T., "The effect of the boundaries on wave propagation in a liquid filed porous solid", *Bull. Seism. Soc. Am.*, 52, 627-638, 1962.

[14] Dey S., De R.K., "Stresses in fluid-saturated porous half-space due to the normal and tangential loadings", *Indian J. Pure and Appl. Math.,* 15, 1375-1397, 1984.

[15] Edelman I., "Bifurcation of the Biot slow wave in a porous medium", *J. Acous. Soc. Amer.*, 114, 90-97, 2003.

[16] Fatt I., "The Biot-Willis elastic coefficients for sandstone", *J. Appl. Mech.*, 2, 296-297, 1959.

[17] Fellah Z. E. A., Fellah M., Lauriks W., Depollier C., "Direct and inverse scattering of transient acoustic waves by a slab of rigid porous material", *J. Acoust. Soc. Amer.*, 113, 1, 1926-1928, 2003.

[18] Fellah Z. E. A., Fellah M., Sebaa N., Lauriks W., Depollier C., "Measuring flow resistivity of porous materials at low frequencies range via acoustic transmitted waves (L)", *J. Acoust. Soc. Amer.*, 119, 4, 61-72, 2006.

[19] Feng S., Johnson D. L., "High-frequency acoustic properties of a fluid/porous solid interface. II. The 2D reflection Green's function", *J. Acous. Soc. Amer.*, 74, 915-924, 1983.

[20] Geerstma J., Smit D.C. "Some aspects of elastic wave propagation in fluid-saturated porous solids", *Geophysics*, 26, 169-181, 1961.

[21] Gradshteyn I.S., Ryzsik I.M., "Table of Integrals, Series, and Products", Fifth edition, ed. Alan Jeffrey. Academic Press, 1994.

[22] Gubaidullin A. A., Kuchugurina O. Y., Smeulders D. M. J., Wisse C. J., "Frequency-dependent acoustic properties of a fluid - porous solid interface", *J. Acous. Soc. Amer.*, 116, 1474–1480, 2004.

[23] Halpern M., Christiano P., "Response of poroelastic halfspace to steady-state harmonic surface tractions", *Int. J. Numer. Anal. Geomech.*, 10, 6, 609-632, 1986.

[24] Kaishin Liua, Ying Liu, "Propagation characteristic of Rayleigh waves in orthotropic fluid-saturated porous media", *Journal of Sound and Vibration,* 271, 1–13, 2004.

[25] Kelder O., Smeulders D.M.J., "Observation of the Biot slow wave in water-saturated Nivelsteiner sandstone", *Geophysics*, 62, 1794–1796, 1997.

[26] Lamb H., "On the propagation of tremors over the surface of an elastic solid", *Phil. Tran. of the Roy. Soc. of London*, A203, 1-42, 1904.

[27] Liu Z., De Boer R., "Dispersion and Attenuation of Surface Waves in a Fluid-Saturated Porous Medium", *Transport in Porous Media,* 29, 207–223, 1997.

[28] Mesgouez A., Lefeuve-Mesgouez G., Chambarel A., "Transient mechanical wave propagation in semi-infinite porous media using a finite element approach", *Soil Dynamics and Earthquake Engineering*, 25, 421–430, 2005.

[29] Molotkov L. A., "Sources acting on the free boundary of a porous Biot medium and reflection on this boundary", *J. Math. Sci.*, 111, 5, 3750-3762, 2002.

[30] Nagy P., "Acoustics and ultrasonics. Experimental methods in physical sciences", Academic press, 161-221, 1999.

[31] Nikolaevsky V.N., Vilchinskaya N.A., Lisin V.P., "Slow seismic waves in sand sea-bed sediments", *Oceanology*, 4, 656-663, 1985.

[32] Norris A. N., "Radiation from a point source and scattering theory in a fluid-saturated porous solid," *J.Acoust. Soc. Amer.*, 77, 2012-2023, 1985.

[33] Paul S., "On the displacements produced in a porous elastic half-space by an impulsive line load (no dissipative case)", *Pure and Appl. Geoph.*, 4, 605-614, 1976.

[34] Payne L. E., Rodriguez J. F., Straughan B.,"Effect of anisotropic permeability on Darcy's law", *Math. Meth. Appl. Sci.,* 24, 427-438, 2001.

[35] Peeters M., "Method for measuring reservoir permeability using slow compressional waves". *Patent Application no 09/252,419 attorney file no. 18683-01890*, 1999.

[36] Philippacoupoulos A. J., "Lamb's problem for fluid saturated porous media", Bull. Seism. Soc. Amer., 78(2), 908-923, 1988.

[37] Plona T.J., "Observation of a second bulk compressional wave in a porous medium at ultrasonic frequencies", *Appl. Phys. Lett.*, 36, 259-261, 1980.

[38] Rice J.R., Clearly M.P., "Some basic stress-diffusion solutions for fluid saturated elastic porous media with compressible constituents", *Rev. Geophys. Space Phys.*, 14, 227-241, 1976.

[39] Schanz M., "Material modelling of porous media for wave propagation problems", *Proc. Appl. Math. Mech.*, 2, 404-405, 2003.

[40] Schanz M., Struckmeier V., "Wave propagation in a simplified modelled poroelastic continuum: Fundamental solutions and a time domain boundary element formulation", *Int. J. Numer. Meth. Engng.*, 64, 1816–1839, 2005.

[41] Seimov V.M., Trofimchuk A.N., Savitsky O.A., "Oscillations and waves in layered media", Naukova dumka, Kiev, 1990.

[42] Smeulders D. M. J., van Dongen M. E. H., "Wave propagation in porous media containing a dilute gas-liquid mixture: Theory and experiments", *J. Fluid Mech.*, 343, 351–373, 1997 .

[43] Tajuddin M., "Rayleigh waves in a poroelastic halfspace", *J. Acoust. Soc Amer.*, 75, 3, 682-684, 1984.

[44] Terzaghi K., "Die berechung der durchlassigkeitsziffer des tones aus dem verlauf der hydrodynamischen spannungserscheinungen", *Sitz. Acad. Wissen.*, Wien Math. Naturwiss. Kl., Abt. IIa, 132, 105-124, 1923.

[45] Valiappan S., Tabatabaie J., Zhao C., "Analytical solution for two-dimensional dynamic consolidation in frequency domain", *Int. J. Numer. Anal. Geomech.*, 19, 10, 663-682, 1995.

[46] Veruijt A., "Elastic storage of aquifers", *Flow through Porous Media*, Academic press, New York, 331-376, 1969.

[47] Veruijt A., "Computational geomechanics", Kluwer Academic Publishers, Dordrecht, 1995.

[48] Wilmanski K., "Porous madia at finite strains. The new model with the balance equation for porosity", *Arch. Mech.*, 48, 4, 591-628, 1996.